

AD-A018 629

ACOUSTICAL AND ENGINEERING PROPERTIES OF SEDIMENTS

Donald J. Shirley, et al

Texas University at Austin

Prepared for:

Office of Naval Research

29 October 1975

DISTRIBUTED BY:

NTIS

**National Technical Information Service
U. S. DEPARTMENT OF COMMERCE**

364203

ADA018629

THE UNIVERSITY OF TEXAS AT AUSTIN

ARL-TR-75-58
29 October 1975

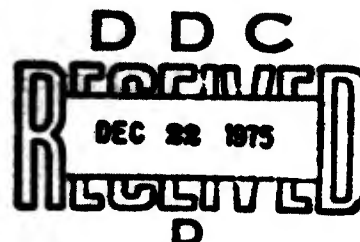
Copy No. 43

ACOUSTICAL AND ENGINEERING PROPERTIES OF SEDIMENTS

Final Report under Contract N00014-70-A-0166, Task 0017
1 August 1973 - 31 October 1975

Donald J. Shirley
Aubrey L. Anderson

OFFICE OF NAVAL RESEARCH
Contract N00014-70 A-0166, Task 0017
NR 083-306



Reproduced by
NATIONAL TECHNICAL
INFORMATION SERVICE
U.S. Department of Commerce
Springfield, VA. 22151

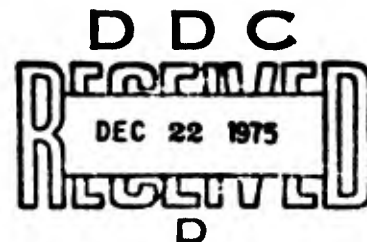
Approved for public release,
distribution unlimited.

ARL-TR-75-58
29 October 1975

ACOUSTICAL AND ENGINEERING PROPERTIES OF SEDIMENTS
Final Report under Contract N00014-70-A-0166, Task 0017
1 August 1973 - 31 October 1975

Donald J. Shirley
Aubrey L. Anderson

OFFICE OF NAVAL RESEARCH
Contract N00014-70-A-0166, Task 0017
NR 083-306



APPLIED RESEARCH LABORATORIES
THE UNIVERSITY OF TEXAS AT AUSTIN
AUSTIN, TEXAS 78712

Approved for public release;
distribution unlimited.

ABSTRACT

As part of a program of in situ acoustical measurements in ocean sediments, an experimental investigation has been started in order to examine the feasibility of measuring shear wave speed, shear wave attenuation, and bulk density by using instruments similar to the compressional wave profilometer previously developed at ARL/UT. Small, rugged shear wave transducers have been developed that have the capability of measuring shear wave speeds as low as 2 m/sec and shear wave attenuation to 520 dB/m in laboratory sediments with shear strength on the order of 10^5 dynes/cm². Measurements were made of the shear wave speed and attenuation in high porosity kaolinite clay as the clay consolidated over a period of time. Water content of the clay was measured during part of the experiment, allowing shear wave speed to be reported as a function of water content.

Experimental and theoretical investigation of the measurement of bulk density by acoustical means indicates that the radiation impedance of a driven piezoelectric ceramic transducer can be determined by measuring the electrical input to the transducer. Preliminary measurements of these parameters are reported.

As an adjunct to the other measurements, physical properties of the sediments used in the laboratory measurements were determined and are reported.

Preceding page blank

TABLE OF CONTENTS

	<u>Page</u>
LIST OF ILLUSTRATIONS	vii
I. GENERAL INTRODUCTION	1
II. SHEAR WAVE MEASUREMENTS	3
A. Introduction	3
B. Transducer Design	4
C. Measurements	11
D. Conclusion	28
III. ACOUSTIC IMPEDANCE MEASUREMENT	33
A. Introduction	33
B. Background	34
C. Measurements	37
D. Conclusion	43
Acknowledgement	45
IV. ENGINEERING PROPERTIES MEASUREMENT	47
A. Introduction	47
B. Grain Size	48
C. Porosity and Bulk Density	52
D. Atterberg Limits	52
E. Vane Shear Strength	53
F. Conclusion	57
V. SUMMARY	59
APPENDIX I	63
BIBLIOGRAPHY	67

Preceding page blank

LIST OF ILLUSTRATIONS

<u>Figure</u>	<u>Title</u>	<u>Page</u>
1	Shear Wave Transducer	5
2	Ceramic Bimorph Element	9
3	Shear Wave Transducer Utilizing Bimorph Elements	12
4	Shear Wave Propagation on Lucite Rod Using Bimorph Transducers	13
5	Shear Wave Propagation in Black Carbonate Clay	15
6	Shear Wave Measuring Apparatus	17
7	Shear Wave Speed versus Time for Kaolinite Clay	21
8	Shear Wave Speed versus Time for Kaolinite Clay	22
9	Amplitude versus Shear Wave Speed for Kaolinite Clay	23
10	Attenuation Coefficient versus Shear Wave Speed	25
11	Shear Wave Propagation in Kaolinite Clay	26
12	Shear Wave Speed versus Time for Kaolinite	27
13	Fractional Water Content versus Time for Kaolinite	29
14	Shear Wave Speed versus Water Content for Kaolinite	30
15	Series Equivalent Circuit for a Piezoelectric Ceramic Transducer	35
16	Admittance Plot for a Piezoelectric Ceramic Transducer	39
17	Output of Acoustic Impedance Probe	41
18	Schematic Diagram of Acoustic Impedance Measuring Circuit	44
19	Grain Size Distribution for Black Clay Sediment	50
20	Grain Size Distribution for Kaolinite Sediments	51
21	Schematic Representation of Vane Shear Apparatus	54
22	Vane Shear Strength of 80% Kaolinite - 20% Silt at 25.8% Water	55
23	Vane Shear Strengths for Laboratory Sediments	56

Preceding page blank

I. GENERAL INTRODUCTION

In an ongoing effort to determine the definitive acoustic parameters of ocean bottom sediments in situ, a program was instituted at Applied Research Laboratories, The University of Texas at Austin (ARL/UT), to measure shear wave speed and attenuation in a manner similar to that of the compressional wave profilometer previously developed and reported (Shirley and Hampton, 1972; Shirley and Anderson, 1973; Shirley et al., 1974), as well as to determine sediment bulk density by measuring the radiation impedance of a driven compressional wave transducer. The program also involved measurement of the engineering properties of the sediments used in the other studies. Preliminary work on all aspects of the program have been reported previously (Shirley and Anderson, 1975b). This report will involve only those results not previously reported. A transducer configuration that allows measurements to be made in high porosity sediments (shear moduli $\sim 10^5$ dynes/cm²) over pathlength of 5 to 10 cm has been developed. These transducers have been used to make measurements of shear wave speed and attenuation in laboratory sediments. Shear wave speeds as low as 2 m/sec and attenuation coefficients as high as 520 dB/m have been measured. At present the transducers exhibit sensitivity to ambient acoustical noise which limits their usefulness for in situ measurements. However, future work in this area is aimed at reducing this noise sensitivity and then proceeding to in situ measurements.

Improvement in capabilities to make acoustical measurement of a sediment bulk density has progressed to the point that measurement of the parameter has been made in laboratory sediments. This was done by measuring the phase angle between the voltage and current waveforms of a transducer in contact with the sediment that is driven at a constant frequency. Observed data indicate, however, that, as expected, this

measurement is sensitive to parameters other than ρc , especially to ambient temperature. Transducer theory indicates that if the driving frequency is varied in order to maintain the transducer at resonance and if the driving voltage is kept constant, then the amplitude of the current waveform will reflect the value of radiation impedance seen by the transducer. Indications are that this type of measurement will be less sensitive to parameters other than the radiation impedance.

Measurements of engineering properties have proceeded in step with the acoustical laboratory measurements. All laboratory sediments used in the acoustical program have been analyzed and characterized by measuring such parameters as grain size, Atterberg limits, water content, and vane shear strength. This part of the program will continue as new sediments are utilized, especially when in situ work is done in natural sediments.

II. SHEAR WAVE MEASUREMENTS

A. Introduction

The measurement of shear wave speed and attenuation is important in the study of acoustics of sediments because as few as five acoustic parameters are usually sufficient to characterize the sediment. For example, if compressional wave speed (C_p) and attenuation (α_p), shear wave speed (C_s) and attenuation (α_s), and bulk density (ρ) are measured, then other parameters such as bulk modulus, shear modulus, and Poisson's ratio can be calculated. Because the measureable parameters of a sediment are easily disturbed and changed in the process of sampling and removal from the ocean bottom, measurements are best made in situ. Toward this end, the ARL compressional wave profilometer was developed to measure compressional wave speed and attenuation during the process of sediment coring. Although some disturbance of the sample occurs during coring, measurement of the acoustical parameters at the lower end of the corer while it is penetrating the bottom (the first part to penetrate the bottom) minimizes the influence of the disturbance in comparison with measurements made after the core is retrieved aboard ship.

After successful implementation of the compressional wave measuring device (Shirley et al, 1974), the feasibility of developing a similar device to measure the shear wave parameters of a sediment was investigated³. Although existing transducer technology was sufficient to implement the compressional wave measurement, no such technology existed for the measurement of shear waves in sediments.

B. Transducer Design

There are several methods that can be used to generate shear waves in a solid. Figure 1 shows a schematic representation of one type of shear wave transducer. As an electrical signal is impressed across the electrodes, the material of the transducer is deformed in a manner illustrated by the dotted lines in the figure. If one of the element faces which experiences transverse motion due to the deformation is in contact with a solid medium, a shear wave will be propagated in a direction perpendicular to the motion of the element face. An AC cut quartz crystal or a piezoelectric ceramic that is polarized perpendicular to the applied field can be used for this type shear wave transducer. Because a transducer of this type exhibits reciprocity, it can be used both to generate and to detect shear waves.

There are two drawbacks to using this type transducer to measure shear waves in sediments and they are listed below.

- (1) The lowest possible frequencies are desirable for such measurement because the attenuation of acoustic energy in a sediment increases with increasing frequency. It is difficult to generate low frequency shear waves with this transducer type because the shear wave element acts as a vibrating bar and the resonance is a function of the bar's stiffness. The transducer element thus requires a large length-to-thickness ratio to have a low resonance frequency.
- (2) The amount of mechanical motion that can be transferred from the element to a sediment is small because the element exhibits a small movement with large force, whereas the sediment is highly compliant and exhibits large movement with small applied force (i.e., there is a large mismatch between the characteristic impedance of the element and that of the sediment).

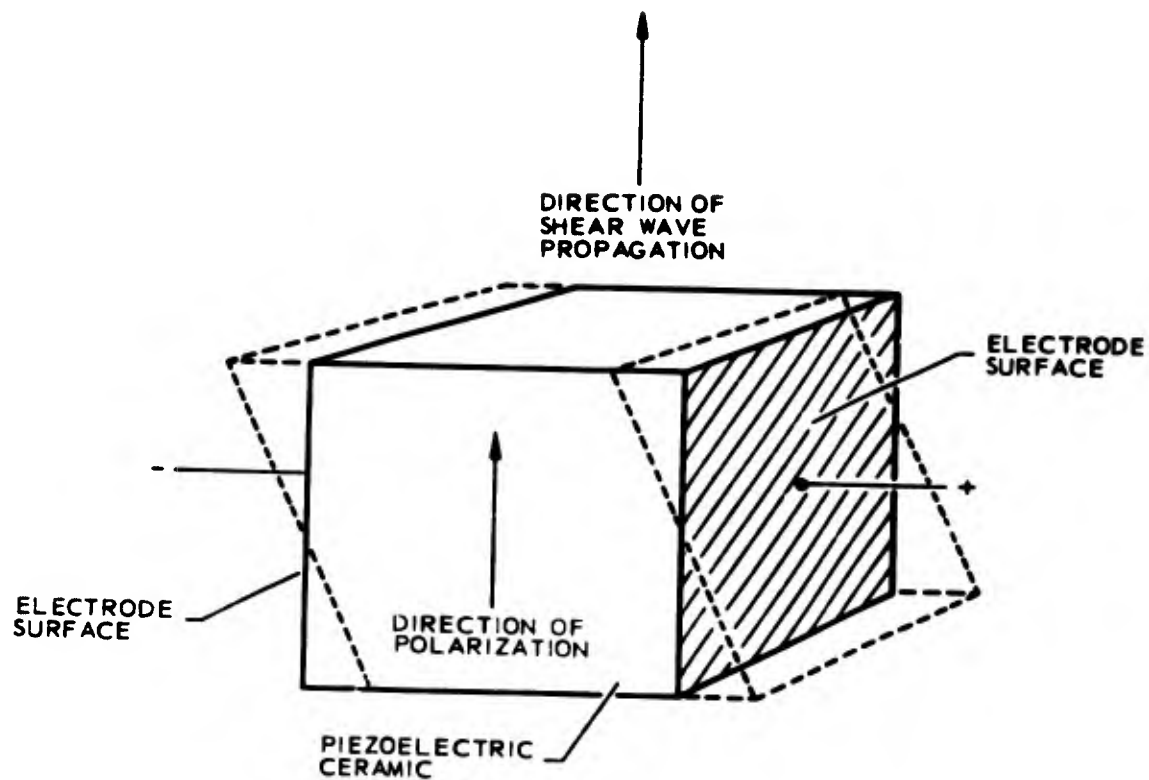


FIGURE 1
SHEAR WAVE TRANSDUCER

ARL - UT
AS-75-473
DJS - DR
4 - 3 - 75

In a preliminary effort to overcome these disadvantages (Shirley and Anderson, 1975), the basic shear element was modified by dividing the element into thin slices to decrease the stiffness and increase the compliance. This modification resulted in a 34.5 dB increase in amplitude for a sliced element when compared to a solid element of the same size. However, even with this improvement work could be done only in sediments with shear moduli of 3×10^7 dynes/cm² or greater (Shirley and Anderson, 1975).

Because work with more realistic sediments (with shear moduli in the range of 10^5 to 10^6 dynes/cm²) was necessary, a better way of generating shear waves was sought.

For a piezoelectric transducer element operated well below resonance, the piezoelectric constant d is defined as

$$d_{ij} = \frac{\text{mechanical strain developed}}{\text{applied electric field}},$$

where the d_{ij} are the terms of a 3×3 matrix. The first subscript defines the applied voltage field direction and the second defines the resultant strain direction. The numbers 1, 2, and 3 refer to the perpendicular coordinate axes, while numbers 4, 5, and 6 refer to rotations about these axes. The No. 3 direction is usually the direction of polarization of the ceramic. Thus, for a shear transducer the appropriate constant is d_{15} , which indicates a voltage applied perpendicular to the direction of polarization and which results in a rotation about the axis perpendicular to both the field and polarization directions. From the definition of the piezoelectric constant, the mechanical strain is related to the applied voltage as follows,

$$d_{15} = \frac{\theta}{V/T},$$

where

θ is the rotation angle and thus the resultant strain,

V is the applied voltage, and

T is the thickness across which the voltage is applied.

The amount of movement D of the shearing face of the transducer is related to the angle as follows,

$$D = L \tan \theta \quad ,$$

where L is the length in the No. 3 direction (direction of polarization).

Combining the two expressions above results in the following relation between the movement D and the other measurable parameters,

$$D = L \tan \frac{V d_{15}}{T} \quad .$$

For the solid element transducer described above, the transducer element parameters are listed below:

$$L = 1 \text{ in.} = 2.54 \text{ cm}$$

$$T = 1/2 \text{ in.} = 1.27 \text{ cm}$$

$$d_{15} = 2.45 \times 10^{-8} \text{ cm/V.}$$

Thus, for V=100 V, the resulting displacement is

$$D = 4.9 \times 10^{-6} \text{ cm.}$$

If the same size (1/2 in. thick) element is composed of four 1/8 in. thick slices instead of a solid block, then the transducer parameters for this element are as listed below.

$$\begin{aligned} L &= 1 \text{ in.} = 2.54 \text{ cm} \\ T &= 1/8 \text{ in.} = 0.317 \text{ cm} \\ d_{15} &= 2.45 \times 10^{-8} \text{ cm/V.} \end{aligned}$$

An applied voltage of $V=100$ produces a displacement of

$$D = 2.0 \times 10^{-5} \text{ cm} ,$$

which is an increase of approximately 12 dB in amplitude. However, because these transducers are operated close to resonance and because the layered transducer has a lower resonance frequency (where attenuation in the medium is less), an even larger amplitude advantage is provided by the layered transducer design.

Further increases in displacement D and reductions in resonance frequency can be obtained by using ceramic bender bimorph elements in a shear wave transducer. Two such elements are operated back-to-back as shown in Fig. 2. The voltage is applied so that one element is expanding while the other is contracting, which results in a force tending to bend the composite element. For this type element, the appropriate piezoelectric constant is d_{31} because the electric field is applied in the direction of polarization; however, the resultant strain of an individual element is along the length of the element. The displacement of the end of the bimorph element, transverse to the individual element displacement, is given by

$$D = \frac{3}{2} d_{31} \frac{L^2 V}{T^2} .$$

Parameters for such a bimorph transducer are listed below,

$$\begin{aligned} L &= 1 \text{ in.} = 2.54 \text{ cm} \\ T^2 &= 1/8 \text{ in.} = 0.317 \text{ cm} \\ d_{31} &= -5.8 \times 10^{-9} \text{ cm/V} . \end{aligned}$$

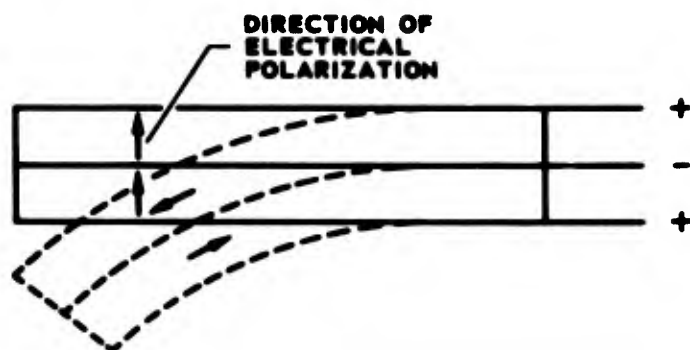


FIGURE 2
CERAMIC BIMORPH ELEMENT

ARL - UT
AS-75-1168
DJS - DR
8 - 20 - 75

For a bimorph transducer with the above parameters, a voltage of $V=100$ V, results in displacement

$$D = 5.6 \times 10^{-3} \text{ cm} .$$

This displacement is about a 9 dB increase over the displacement of the layered shear plate. However the resonance frequency of the bimorph is much lower.

For the shear plate, the resonance frequency, f , is given by

$$f = \frac{F}{L} ,$$

where F is the frequency constant of the ceramic material. For the ARL transducer $f \approx 79/1 = 79$ kHz for the shear plate. Conversely, for the bender bimorph, the resonance frequency is described by

$$f = \frac{FT}{L^2} ,$$

so

$$f \approx \frac{(31)(1/8)}{(1)^2} = 4 \text{ kHz} ,$$

for the bimorph. Because of its inherently large mechanical motion and its low resonance frequency, the bimorph was chosen as the appropriate element for use in a shear wave transducer for sediment work.

To use the bimorph element to generate shear waves, the propagation medium is placed in contact with one end of the element. As the bimorph bends back and forth in response to an electrical driving signal, the transverse motion of the end of the element generates shear waves in the portion of the medium in contact with the moving end. The bimorph

must be made as thin as possible to increase amplitude and decrease resonance frequency; therefore, an array of bimorph elements, separated by a layer of high compliance material, is used to increase the area of the radiating surface. Such a bimorph array is illustrated in Fig. 3. Here there are three bimorphs in the array, each of which is $1/8$ in. thick, $1/2$ in. wide, and 1 in. long. Corprene sheets of $1/16$ in. thickness are used to separate the individual bimorphs of the array. The dimensions of the total array are then $1/2$ in. x $1/2$ in. x 1 in.

C. Measurements

Bimorph transducers were cemented to each end of a 2 in. diam by 1 m long plexiglass rod. This rod was selected as the propagation medium to be used to compare the different types of shear wave transducers (Shirley and Anderson, 1975) because it exhibits essentially constant propagation parameters which a laboratory sediment would not. Figure 4 shows an oscilloscope photograph of the received waveforms. A maximum amplitude was obtained at 1.67 kHz. With no preamplifier, the output from the element was 2.5 Vp-p, with a projector drive level of 500 Vp-p, which is 15 dB better than any other type of transducer tested. The maximum at 1.67 kHz probably does not represent the resonance frequency of the transducer, but rather represents the breakover point between increasing output from the transducers and increasing attenuation in the plastic rod. The system provided usable signal levels from about 70 Hz where the signal was obscured by noise up to about 10 kHz, at which point the compressional waves from the device interfered to obscure the shear waves.

To determine whether the transducer system would operate satisfactorily in a sediment, the transducers were mounted diametrically opposite on a stainless steel cylinder so that the separation between transducer faces was 1.92 in. (4.88 cm); the cylinder was then filled with sediment. The projector was driven by a single cycle pulse with a peak-to-peak amplitude of 600 V and a frequency of 338 Hz. The signal from the receiver was amplified by 40 dB, was filtered by a

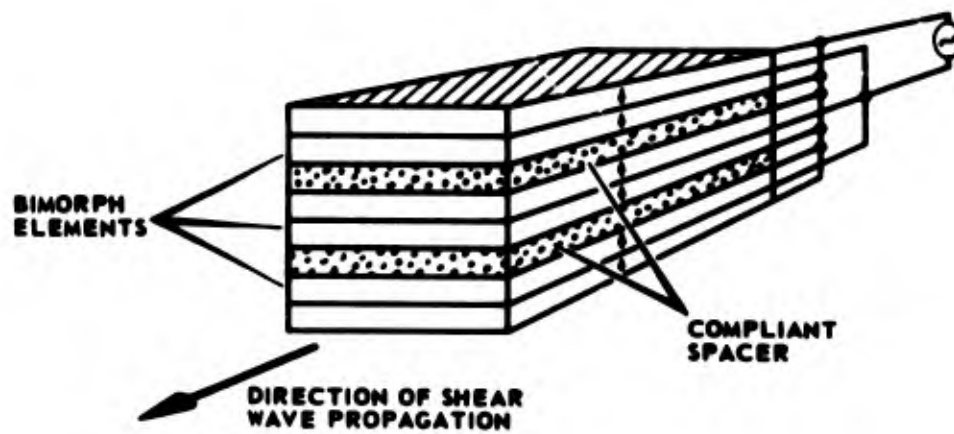


FIGURE 3
SHEAR WAVE TRANSDUCER
UTILIZING BIMORPH ELEMENTS

ARL - UT
AS-75-1169
DJS - DR
8 - 20 - 75

VERTICAL SCALE: 0.5 V/div
HORIZONTAL SCALE: 1 msec/div
 $f_0 = 1.67 \text{ kHz}$

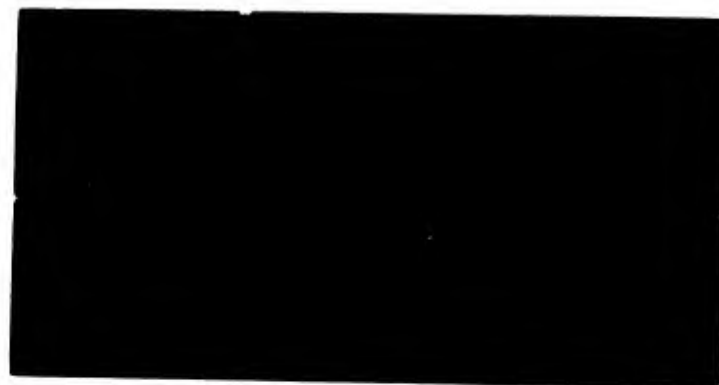


FIGURE 4
SHEAR WAVE PROPAGATION ON LUCITE
ROD USING BIMORPH TRANSDUCERS

200 to 1500 Hz bandpass filter, and was displayed on an oscilloscope. Figure 5 shows an oscilloscope photograph of the output when a black soil with 63.8% water (% water = wt. of water/wt. of solids + water \times 100) and wet bulk density of 1.29 g/cm³ was used as the propagation medium. The shear wave is the large pulse on the trace starting 13.5 msec after the beginning of the transmit pulse. By using the 4.88 cm separation between transducers, a shear wave speed of 3.6 m/sec is calculated. The low amplitude, higher frequency pulse at the start of the trace is the residual of a much larger signal that has been nearly eliminated by the bandpass filter. This precursor pulse is generated at the start and end of the low frequency driving signal and has a frequency of about 9.7 kHz. The pulse travels as a compressional wave around the circumference of the steel cylinder. This energy is probably due to thickness mode vibration of the transducer array, and propagation of the resultant compressional wave energy will occur perpendicular to the direction of propagation of the shear waves.

By using the relationship

$$\mu = \rho C_s^2$$

where μ is the shear modulus and ρ the bulk density of the medium, a value of 1.67×10^5 dynes/cm² is calculated for the shear modulus of the clay. This calculation confirms that the transducers can be used to make measurements in naturally occurring clays and muds which have a shear modulus range of 10^5 to 10^9 dynes/cm² (Anderson, 1974).

As yet the only sediment that has been used extensively for shear wave propagation is the pure kaolinite clay. It was felt that the kaolinite had more uniform and easily understood physical properties than any of the other sediments that were available for these experiments.

VERTICAL SCALE: 5 mV/div
HORIZONTAL SCALE: 5 msec/div
40 dB GAIN
 $f_0 = 338 \text{ Hz}$



FIGURE 5
SHEAR WAVE PROPAGATION
IN BLACK CARBONATE CLAY

ARL - UT
AS-75-1320
DJS - DR
10 - 3 - 75

After development of the bimorph shear wave transducer, a program was started to measure shear wave speed and attenuation in laboratory mixed sediments. For an accurate measurement of shear wave speed, both the spacing between transducers and timing of pulses must be accurately known. To facilitate these measurements, a chamber was constructed so that the transducer spacing could be measured with a micrometer. Figure 6 shows a schematic drawing of the chamber, which consists of a cylindrical aluminum pot 4 11/16 in. i.d. by 8 in. high, with 5/8 in. thick walls. Transducers were affixed in diametrically opposed holes through the walls of the cylinder 3 in. above the bottom of the chambers. The receiving transducer was rigidly fixed, while the projector was mounted on the end of a smaller cylinder which could be moved radially in and out of the larger cylinder by a micrometer positioning device that was accurate to 0.001 in. The pot could then be filled with a sediment and the transducers positioned to an accurately known spacing.

Time delay information was obtained by using a 2-channel oscilloscope to display the received signal along with a variable length square pulse which started in coincidence with the start of the transmit pulse. By using the end of the square pulse as a cursor which could be lined up with an easily identifiable feature of the received pulse, the time delay to that particular feature could be determined by measuring the period of the pulse with a frequency counter. In actual practice the difference in time delay to a feature on the received pulse and to the same feature on the electrical feedover pulse from the projector was used to calculate shear wave speed. In this way, any inaccuracies due to distortion of the received pulse in the filter or the other electronics could be eliminated since the received pulse is almost an exact replica of the electrical signal applied to the projector transducer and since both the electrical feedover and the received pulse must travel through the same electronics circuits before being displayed on the oscilloscope.

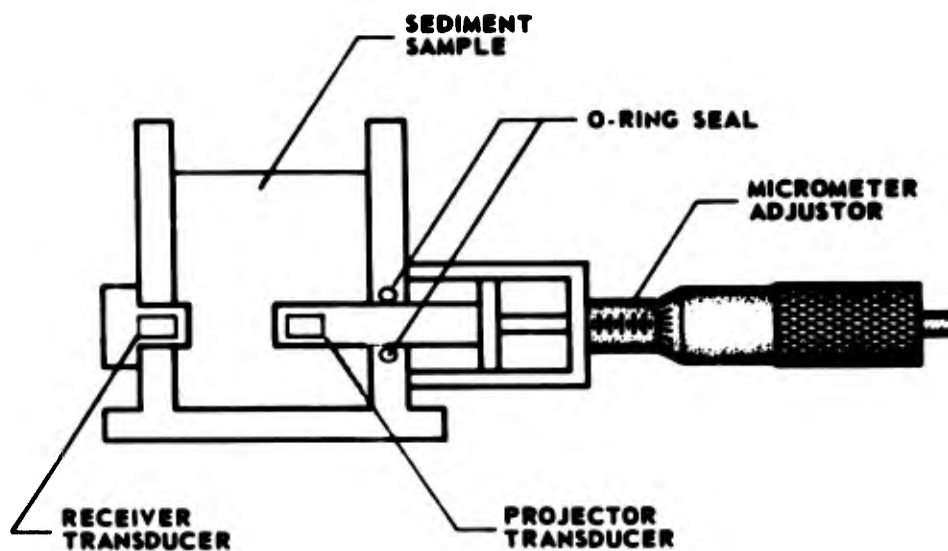


FIGURE 6
SHEAR WAVE MEASURING APPARATUS

ARL - UT
AS-75-1321
DJS - DR
10 - 3 - 75

Use of this method of time delay measurement gives a repeatability of about $\pm 1.6\%$ for a 3 to 4 msec time delay.

At this point, the noise levels encountered in these measurements should be described. In a quiet environment with few contributions from such sources as footsteps, speech, air conditioning noise, etc., the received shear wave pulse is usually several decibels above the background, as illustrated in Fig. 5. However, noise in the environment can easily become large and can obscure the shear wave signal. This sensitivity to ambient noise severely limits the usefulness of the present transducer configuration and, because the ambient noise is in the same frequency range as the operating frequency, the band-pass filter cannot be used to eliminate it. One proposed solution to this problem is to use two receiving elements, one in contact with the medium to receive shear waves and the other isolated so that it will not respond to shear waves but will respond to any ambient noise. With the elements electrically connected so that their outputs oppose, the common mode ambient noise will cancel but the received shear wave pulse will not. This solution has not yet been implemented.

One of the most straightforward methods of measuring the speed and attenuation of an acoustic wave is to measure the time delay and amplitude of the received pulse at several different transducer spacings. A plot of time delay versus separation would then yield a straight line whose slope is the speed of the acoustic wave. A plot of amplitude versus separation (with corrections for spreading loss) would similarly yield the attenuation coefficient. However, when an attempt was made to measure the shear wave speed and attenuation in this manner, it was found that any movement of the transducers disturbed the sediment and caused erroneous readings. If the transducers were either moved together or separated, the time delay always

increased, which indicates a slower shear wave speed. This suggests that the sediment frame was being fractured by the transducer motion, thus lowering the shear modulus of the material.

One alternative to the above procedure is to leave the transducers fixed so that the sediment is not disturbed. By measuring the separation of the transducers and the time delay, the shear wave speed can be calculated. The accuracy of this method is limited by the ambiguity in measurement of separation of transducers resulting from the finite thickness and unknown shear wave speed of the transducer window material. The resulting error is small because the window thickness is small (approximately 1/16 in.) in comparison to the sediment path length (from 3 to 4.5 in.). Another feature of this fixed transducer method is that it requires standardized calibration media of known attenuation if shear wave attenuation is to be measured.

An alternate procedure, which is essentially a combination of both the previously discussed methods, is to use one fixed projector transducer in conjunction with two or more receiving transducers fixed at different spacings. The time delay of each received pulse can then be plotted versus the measured spacing for that particular transducer to yield a line of slope equal to the shear wave speed. Similarly, attenuation measurements can be made by correcting the relative signal level from the two receivers for spreading loss and for individual receiver sensitivities. This procedure has required extensive modification of the existing laboratory apparatus, but the increased accuracy was felt to justify the action.

The second of the three methods described above (fixed projector and single receiver) was used to make shear wave measurements in the pure kaolinite clay. The dry clay was mixed with water and thoroughly blended with a drink mixer to form a very liquid mixture. This liquid mixture was then subjected to a vacuum for several hours to remove any entrained air. The mixture was then poured into the transducer

apparatus shown in Fig. 6, and also described above. The projector transducer was backed out as far as it could be, and the clay-water mixture was again stirred with a rod to ensure a homogeneous mixture. The projector transducer was then moved to a selected position and timing was started. Hourly readings were made for the first few hours; then, as the clay became increasingly dense through the action of gravity and interparticle attraction, readings were made at increasing time intervals. The measurements were made over a period of about 150 h at three different transducer spacings: 9.75 cm, 8.48 cm, and 7.21 cm. In Fig. 7 the resulting measured values of shear wave speed versus time are shown. Zero time on the plot was actually 20 min after the clay was stirred. For each successive run the clay was restirred in the container to the same consistency as at the start of the initial run. The shear wave speeds are not the same for each run, but the data for each run define a relatively smooth wave with only small scatter. The most disagreement in shape of the curves occurs at the start of each run. This disagreement is easily seen in Fig. 8, where the scales have been expanded for the same data that are shown in Fig. 7. The peculiar behavior of the shear wave speed in the first hour becomes more pronounced as the transducers are positioned closer and closer together. This behavior is possibly due to the transducers compressing the sediment frame during initial setup for the measurements; thus a higher initial shear wave speed than would be normal would be caused. As time progresses, the excess frame pressure from the transducers relaxes and eventually disappears, so that the curve assumes its normal shape after about 2 h.

Attenuation data were taken on the same runs as the speed by recording the amplitude of the received pulse (Fig. 9). Figure 9 shows the amplitude of the shear wave pulse plotted against the shear wave speed as the speed changed with time due to consolidation of the sediment. The solid lines in Fig. 9 are empirical fits to the data. Attenuation coefficients can be calculated for each value of shear wave speed by using values from the three curves and the physical

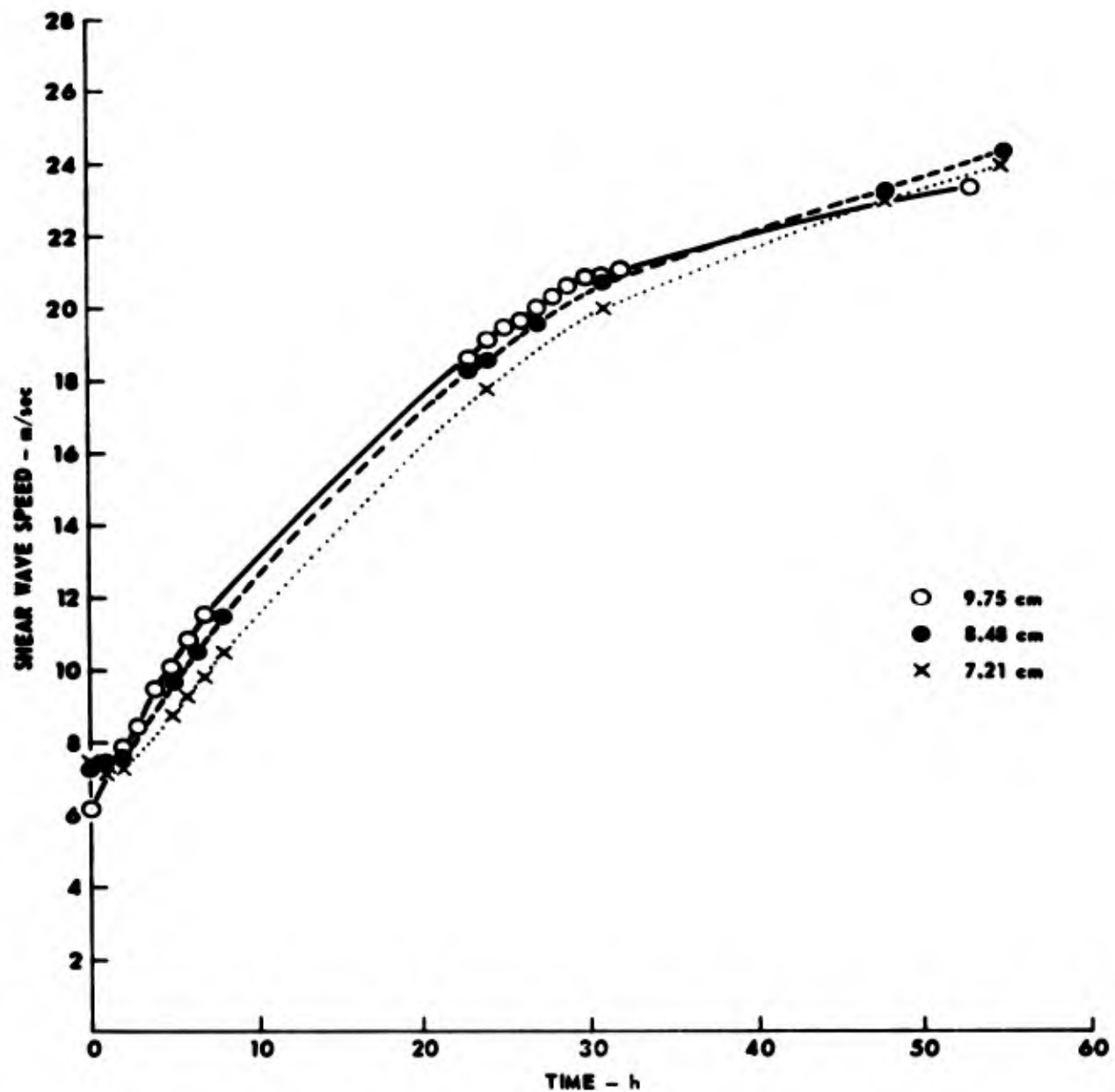


FIGURE 7
SHEAR WAVE SPEED VERSUS TIME FOR KAOLINITE CLAY

ARL - UT
AS-75-1322
DJS - DR
10 - 3 - 75

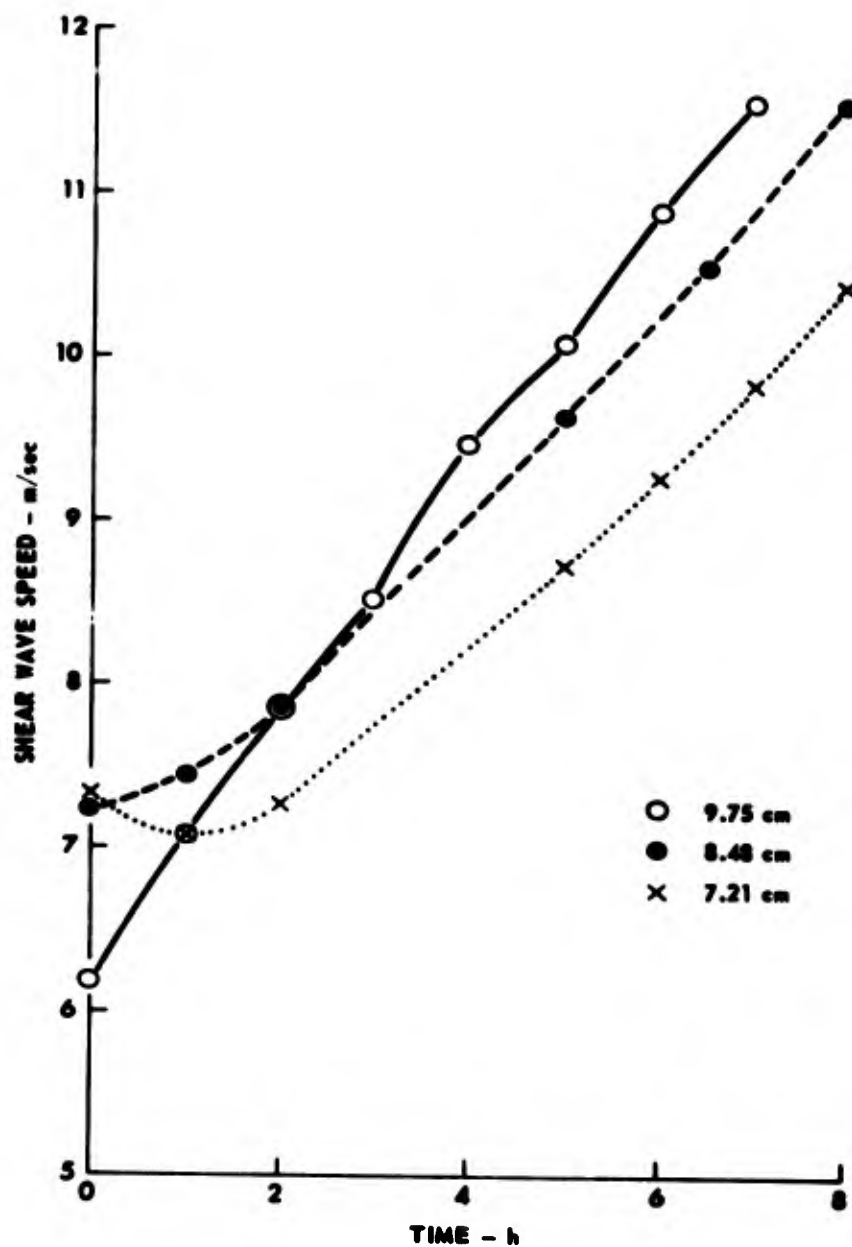


FIGURE 8
SHEAR WAVE SPEED VERSUS TIME FOR KAOLINITE CLAY

ARL - UT
 AS-75-1323
 DJS - DR
 10 - 3 - 75

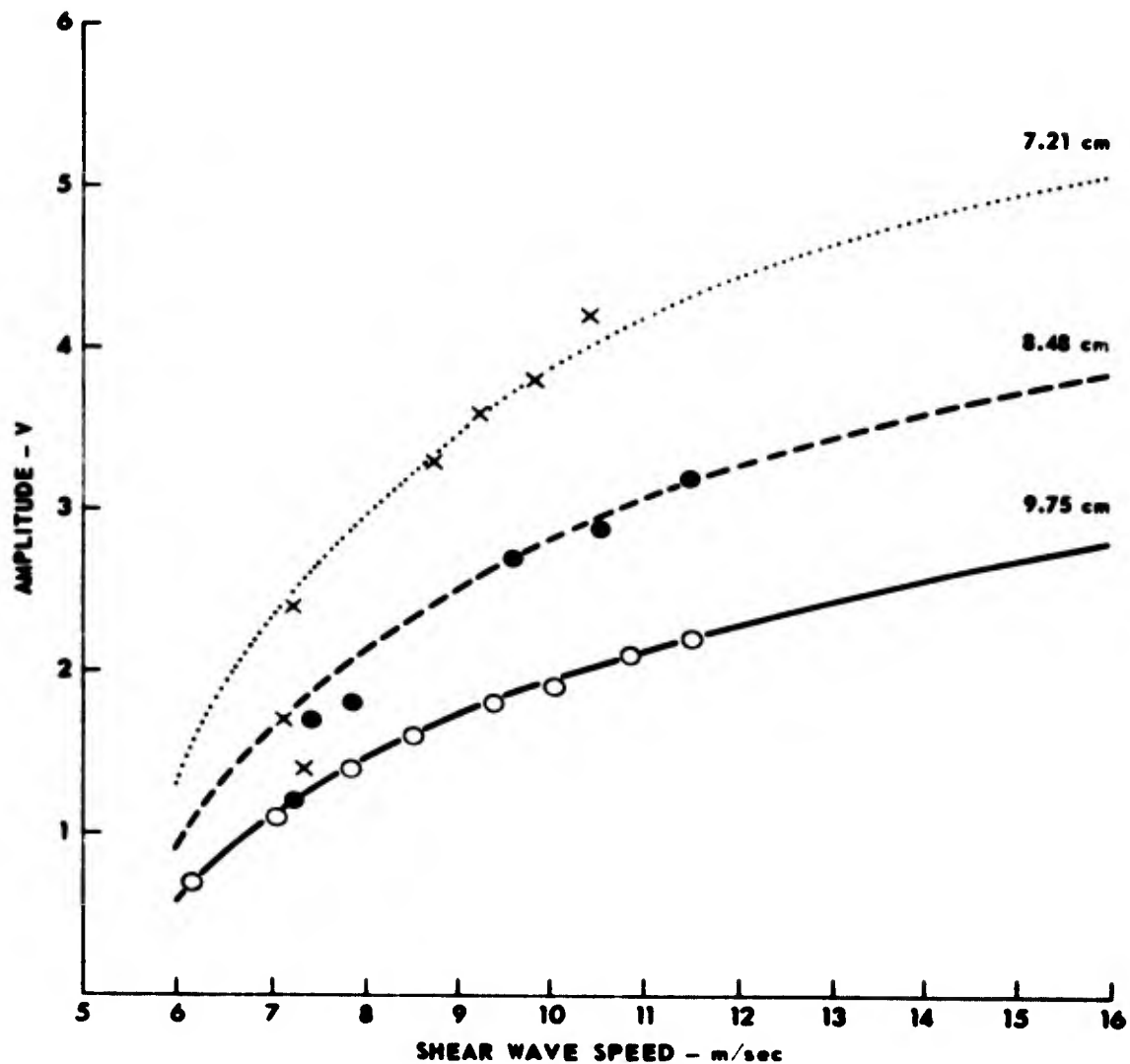


FIGURE 9
AMPLITUDE VERSUS SHEAR WAVE SPEED FOR
KAOLINITE CLAY DURING CONSOLIDATION

ARL - UT
 AS-75-1324
 DJS - DR
 10 - 3 - 75

separation of the elements. Figure 10 shows a plot of resulting values of attenuation coefficient (in decibels/meter) versus shear wave speed. The data exhibit an approximately inverse exponential relationship. The smooth curve is an empirical fit to the data with the equation

$$a = 90 \exp(3.5/c_s) \quad ,$$

where

a - attenuation coefficient in decibels/meter, and
 c_s = shear wave speed in meters/second.

Because the attenuation is so high at shear wave speeds below 6 m/sec, accurate measurements in media with high porosity are not easily made. However, some measurements have been made of shear wave speeds as low as 2 m/sec. Figure 11 shows an oscilloscope photograph of such a low speed shear wave. Signal levels were so low that the pulse could be observed only by making a time exposure with the oscilloscope camera to integrate the noise. With a transducer separation of 6.58 cm and a measured time delay of 33 msec, a shear wave speed of 2 m/sec is calculated. Comparison of the voltage level of this pulse to voltage levels at lower values of attenuation indicate an attenuation coefficient of about 520 dB/m. This coefficient agrees well with an attenuation coefficient value of 518 dB/m, which is predicted by the above empirical expression for a shear wave speed of 2 m/sec.

The square of the shear wave speed is proportional to the shear modulus (μ) and inversely proportional to the bulk density (ρ), both of which are dependent upon the porosity of the sediment. During one series of measurements, the sediment was sampled to determine the water content each time a shear wave speed measurement was made. Figure 12 shows the shear wave speed data versus time for the duration of the test. For the first 100 h of the test, the container was sealed to prevent evaporation of the water. As was previously observed,

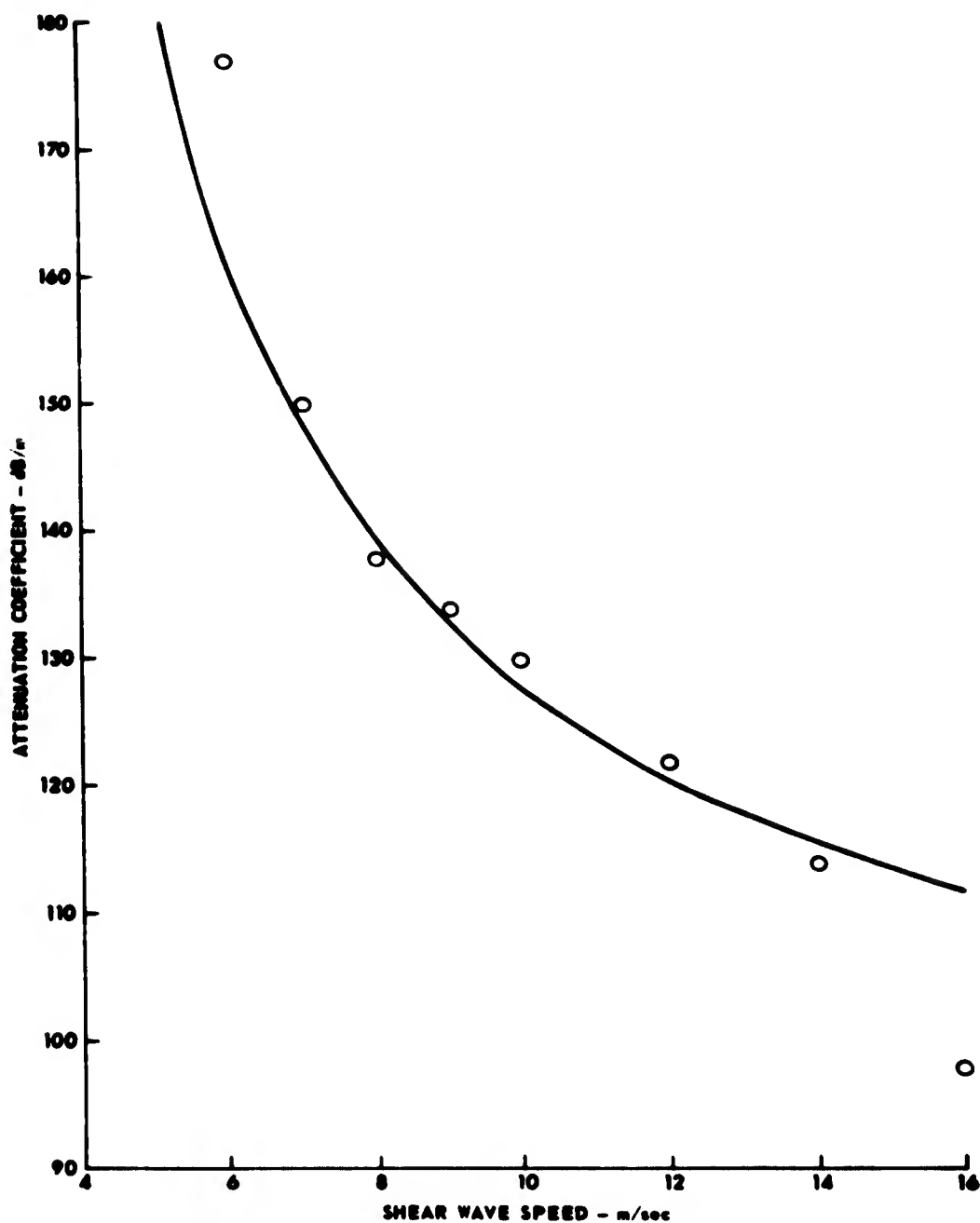


FIGURE 10
ATTENUATION COEFFICIENT VERSUS SHEAR WAVE SPEED
FOR KAOLINITE CLAY DURING CONSOLIDATION

ARL - UT
AS-75-1325
DJS - DR
10 - 3 - 75

VERTICAL SCALE - 0.5 V/div
HORIZONTAL SCALE - 5 msec/div
80 dB GAIN
 $f_0 = 200 \text{ Hz}$



FIGURE 11
SHEAR WAVE PROPAGATION IN KAOLINITE CLAY

ARL - UT
AS-75-1326
DJS - DR
10 - 3 - 75

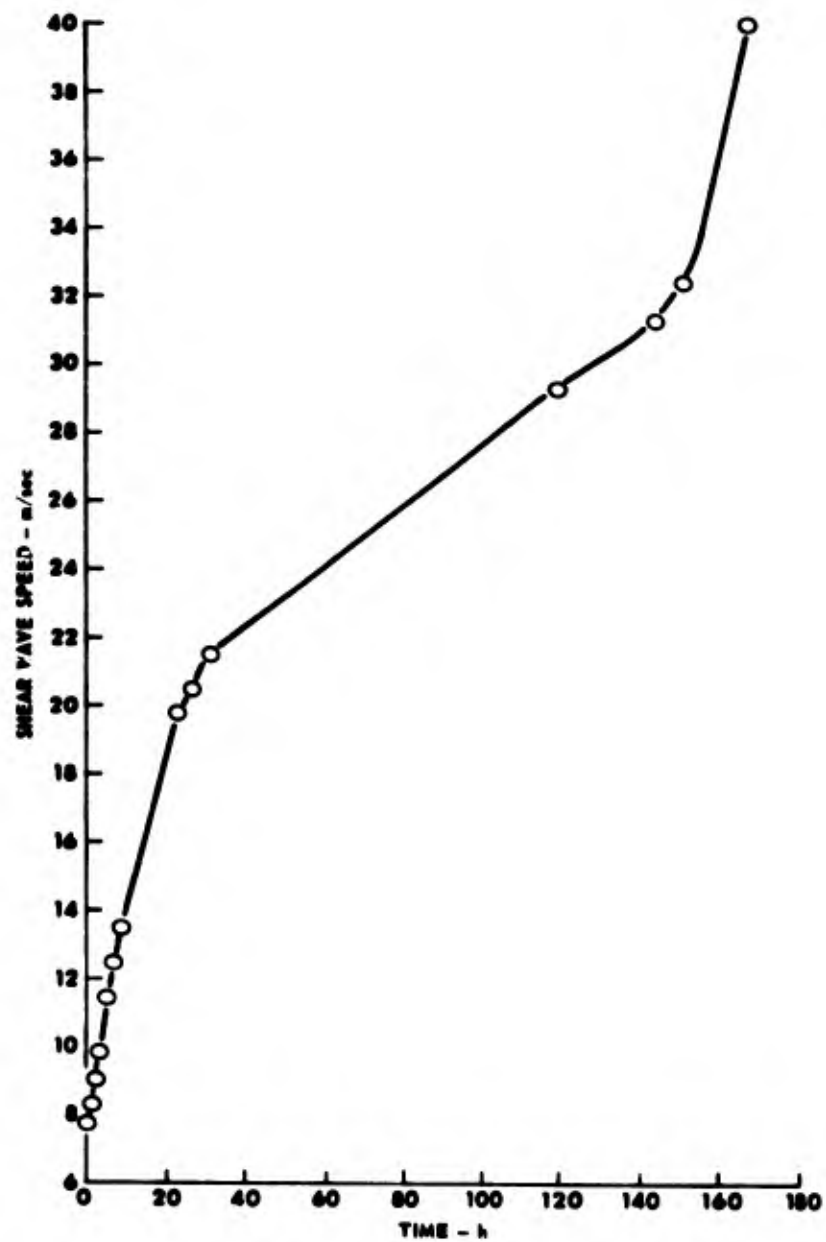


FIGURE 12
SHEAR WAVE SPEED VERSUS TIME
FOR KAOLINITE CLAY

ARL - UT
AS-75-1327
DJS - DR
10-3-75

during this interval the shear wave speed increases smoothly as the clay consolidates under the influence of gravity and interparticle forces (compare the first 30 h in Fig. 12 with Fig. 7). After 120 h, the seal on the container was broken, the excess water was removed from the top of the sediment, and the sediment was allowed to air dry for the remainder of the test. The increased rate of consolidation is reflected in Fig. 12 in the steeper slope of the shear wave speed curve beyond 140 h. Figure 13 shows a plot of the fractional water content in the clay samples for the same time period as Fig. 12. The scatter in the data demonstrates the difficulty of obtaining a good sample from the sediment. The samples were increasingly difficult to take as the clay became stiffer. Also, since there was a gradient of water content in the clay, any inaccuracy in repeating the sampling depth would be reflected as a variation in the apparent water content.

Even when a small sampling tube was used, there is some disturbance of the sediment, as evidenced by a lowered shear wave speed immediately after taking a sample. To eliminate this problem, it may be necessary to determine the sediment density by methods, such as nuclear density probe or by acoustical measurements of α_p , which do not require removal of a sample.

Figure 14 shows the shear wave speed data (from Fig. 12) plotted versus the sediment water content (from Fig. 13). The solid straight line is a least squares fit to the data points. If the linear trend of the data continues to higher water content, the axis intercept at which the speed is zero will be at 56.3% water content. Shear wave speed measurements for the higher water content will require more sensitive transducers and a quieter environment.

D. Conclusion

The objective of this portion of the study has been to develop shear wave transducers suitable for use in determining in situ shear

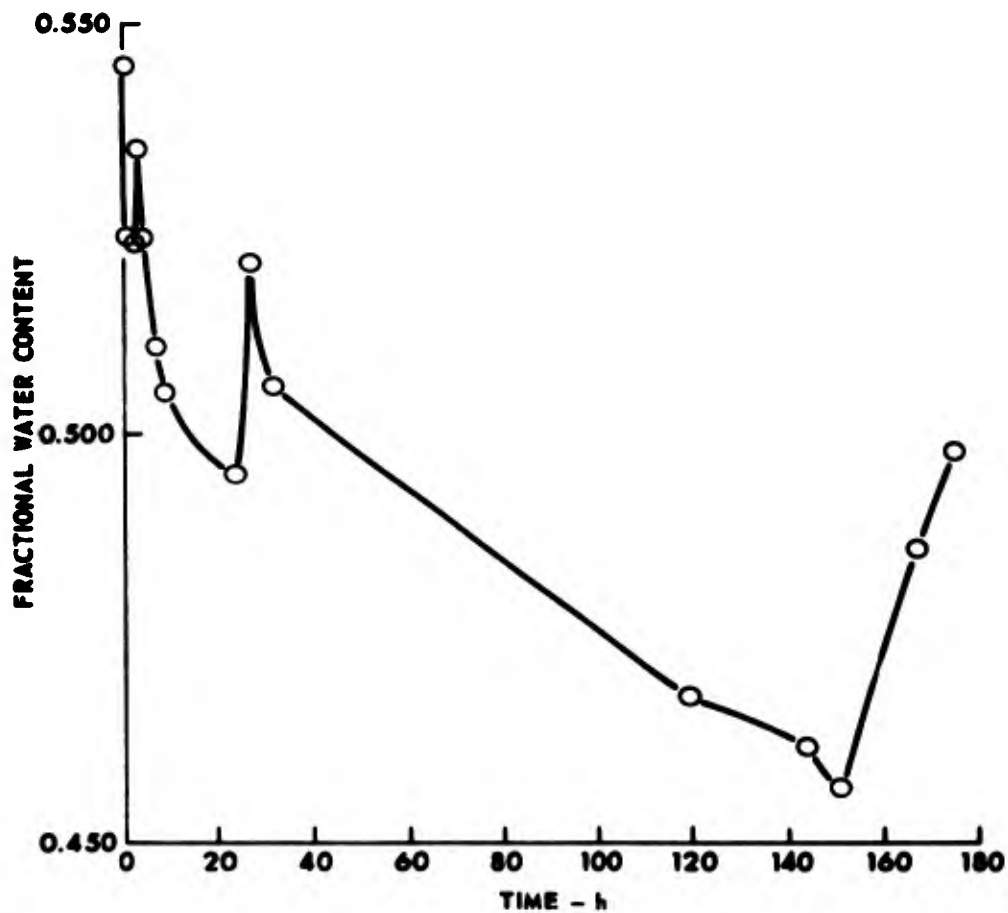


FIGURE 13
FRACTIONAL WATER CONTENT VERSUS TIME
FOR KAOLINITE CLAY

ARL - UT
AS-75-1328
DJS - DR
10 - 3 - 75

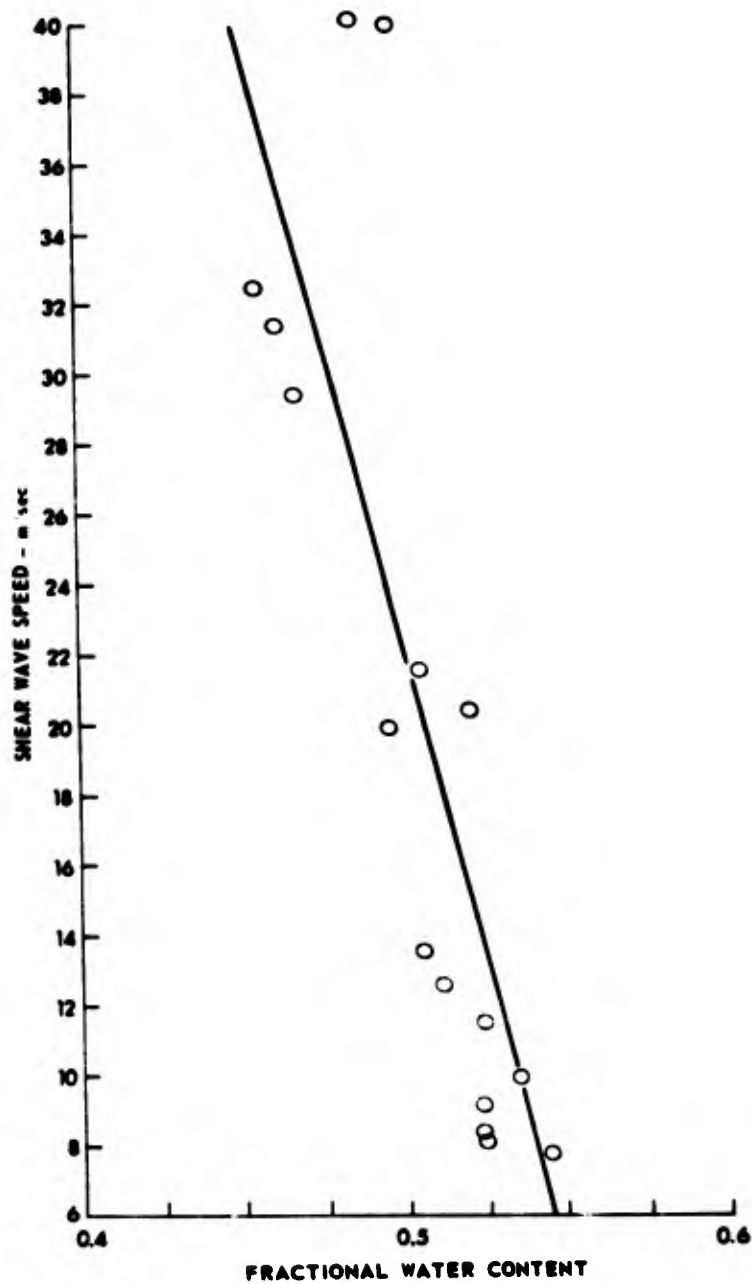


FIGURE 14
SHEAR WAVE SPEED VERSUS WATER
CONTENT FOR KAOLINITE CLAY

ARL - UT
 AS 75-1329
 DJS - DR
 10 - 3 - 75

wave properties of marine sediments. Transducers have been developed which are capable of making these measurements as long as the noise environment is low. Further work is now in progress to increase the signal-to-noise ratio and to utilize other laboratory sediments with different physical parameters for comparison of acoustical properties.

In their present configuration, the transducers are capable of making shear wave speed measurements in a sediment with parameter values as low as a bulk density of 1.38 g/cm^3 , a shear modulus of $5.5 \times 10^4 \text{ dynes/cm}^2$, and a shear wave speed of 2.0 m/sec . With refinements in noise immunity and sensitivity, these limits can be pushed even lower. The next transducer design will include the use of thinner bimorph elements (to increase transducer response) and some provisions for elimination of common mode noise. New transducer design will also include a compressional wave element so that compressional wave speed and attenuation can be measured at the same time and over the same path as the shear wave measurements. Alternate techniques for measurement of bulk density of the sediment are being examined in order to reduce disturbance of the sediment. Techniques under consideration include a nuclear density probe and measurement of the characteristic acoustic impedance of the sediment with a device to be described later in this report.

III. ACOUSTIC IMPEDANCE MEASUREMENT

A. Introduction

In the study of the acoustical properties of sediments, one of the parameters of interest is the sediment bulk density. The bulk density is the weight of a unit volume of the sediment and can be determined by removing an accurately measured volume of sediment and weighing it. However, when sediment is removed from its normal environment, changes in such parameters as pressure and temperature will cause inaccuracies in the measurement of the volume of the material.

What is needed then is a device to measure in situ sediment bulk density without disturbing the sediment. One such device presently in use is the nuclear density probe. With this device the bulk density of the sediment is determined by measuring its opacity to gamma radiation. The nuclear density probe has some disadvantages, however, because the measurement is sensitive to the chemical composition of the sediment and a chemical analysis is required for accurate work (Preiss, 1968a and 1968b). Also there are the inconvenience and hazard involved in handling radioactive material.

Another method of measuring the bulk density of a sediment (ρ) is concurrent measurement of characteristic acoustical impedance (ρc_p) and compressional wave speed (c_p). This measurement can be made by measuring the electrical input to a transducer immersed in the sediment. Changes in the electrical input are caused by variation of the radiation impedance presented to the transducer by changes in ρc_p of the sediment.

Preceding page blank

B. Background

Figure 15 shows a schematic diagram of the series equivalent circuit of a piezoelectric ceramic transducer. In the diagram, c_o is the static capacitance, R_o represents the dissipation in the static capacitance, L and C are the resonant circuit components of the transducer, R_L is the dissipation in the transducer, and R_R is the radiative loading on the transducer. The transformation factor converts the mechanical output parameters to the electrical input parameters. For an ideal transducer, the lumped components L and C and the mechanical parameters M and K are related as follows (Hueter and Bolt, 1955),

$$L = \frac{M}{\alpha^2}$$

and

$$C = \frac{\alpha^2}{K} \quad ,$$

where M is the mechanical mass of the transducer and K is the mechanical stiffness. The radiative load has the relationship

$$R_R = \frac{Z_R}{\alpha^2} \quad ,$$

where Z_R is the mechanical radiation impedance which in general is a complex quantity but which in the special case of large radiation area to wavelength ratio reduces to

$$Z_R = 2\rho_o c_p A \quad ,$$

where A is the radiating area of each transducer face. This relationship holds for radiative coupling from both faces of the transducer. It is

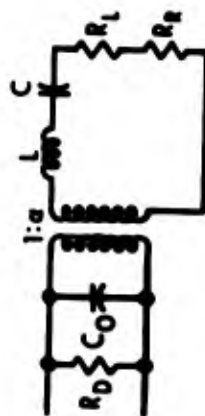


FIGURE 15
SERIES EQUIVALENT CIRCUIT FOR A
PIEZOELECTRIC CERAMIC TRANSDUCER

ARL - UT
AS-75-1330
DJS - DR
10 - 3 - 75

thus apparent that a direct relationship exists between the bulk density ρ_0 of the medium and the radiation impedance of the transducer. This radiation impedance can in turn be measured by determining the transducer admittance from its electrical input parameters.

If one considers the complex admittance of a piezoelectric ceramic transducer

$$Y = G + iB \quad ,$$

where Y is the complex admittance, G the conductance, and B the susceptance, then the relationships between electrical input and radiative output can be more clearly seen. Figure 16 shows plots of the motional admittance for a piezoelectric ceramic transducer. The larger admittance circle is for the transducer loaded by air and the smaller circle is for water loading.

From the admittance circle diagram, the values for the components in the equivalent circuit can be calculated. The height, H , of the center of the circle above the G -axis is given by

$$H = 2\pi f_0 C_0 \quad ,$$

where f_0 is the frequency at the point on the circle intersected by a horizontal line through the center. This frequency is also the resonance frequency for the transducer with that particular loading. From the resonance frequency, and the two frequencies at 90° around the admittance circle from it, one can determine the Q of the circuit and thus can calculate L and C . The diameter (D) of the circle has the relationship

$$D = \frac{1}{R_L + R_R} \quad .$$

For air loading, R_R is essentially zero and

$$D = \frac{1}{R_L} ,$$

so that both the dissipative and radiative loading can be determined by the change in diameter of the admittance circle between measurements with the transducer in air and measurements with the transducer in a medium with finite R_R .

There are problems associated with determining R_L and R_R due to dissipation in the transducer mounting and covering. Here these extra dissipations have been lumped into R_L with the actual dissipation inside the element. As a result, R_R represents only that energy actually dissipated into the medium of interest.

C. Measurements

Table I summarizes the parameters calculated for the particular transducer used to derive the circle plots in Fig. 16. The difference in C_0 between water and air loading reflects changes in external capacitance. However, the change in L resulted both from the fact that the size of the radiation area of the transducer was on the same order as the wavelength so that Z_R was complex and slightly inductive (instead of purely resistive) and from other factors such as a temperature difference for the two media. The transducer used in this case was a PZT disc of 9/16 in. diam by 7/8 in. thick.

In Fig. 16, two straight lines are shown from the origin to points on the respective admittance circles for the same frequency of 65.431 kHz. The respective angles θ_1 and θ_2 then represent the phase angles between the voltage and current waveforms of the electrical input to the transducer at the two different radiation loads for this selected frequency.

TABLE I

	Water Loaded	Air Loaded
C_o	62.26 pF	83.64 pF
L	228.6 mH	79.6 mH
C	25.83 pF	8.61 pF
R_L	1.69 k Ω	1.69 k Ω
R_R	8.51 k Ω	0

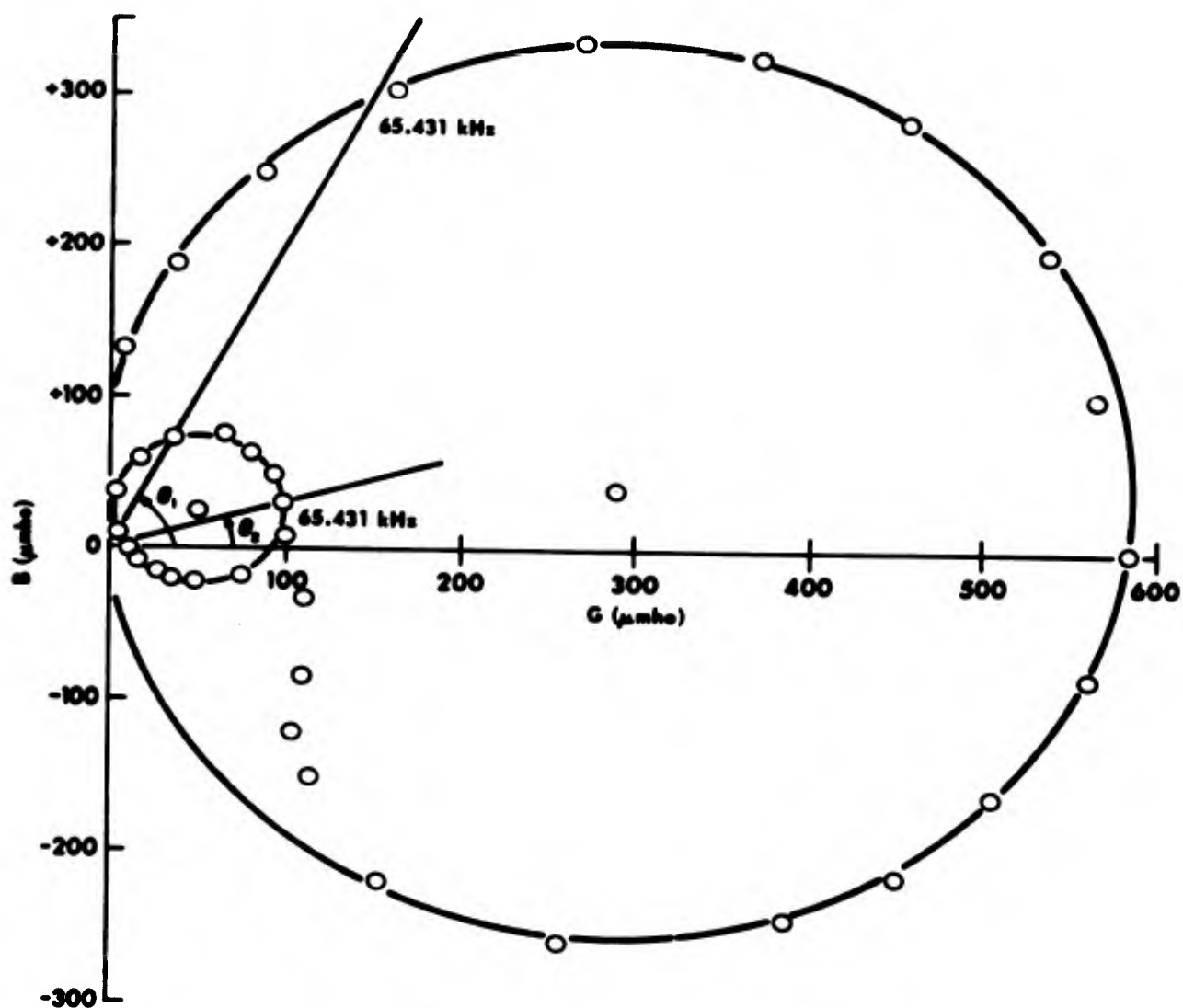


FIGURE 16
ADMITTANCE PLOT FOR A PIEZOELECTRIC CERAMIC TRANSDUCER

ARL - UT
 AS-75-1331
 DJS - DR
 10 - 3 - 75

Neglecting the clamped capacitance C_0 of the transducer, the relationship of phase angle θ to the resistive part of the series equivalent circuit is

$$\theta = \cos^{-1} \frac{R\omega}{\sqrt{(\omega^2 L - \frac{1}{C})^2 + R^2 \omega^2}},$$

where ω is the frequency of the driving waveform, R is the total resistance ($R_L + R_R$), and L and C are the lumped capacitance and inductive components of the equivalent circuit. Thus, though the phase angle between the driving voltage and current waveforms is an easily measured parameter, the relationship between that angle and the radiation resistance is not simple.

If the values for L and C determined for the air loaded case are used to calculate θ , a value of 59° is found for air loading and 16.5° for water loading. The 59° for air loading compares favorably to the measured value of 60.3° (Fig. 16). However, the measured value of 2.5° for water loading disagrees with the value thus calculated. If the correct values of L and C , for the water loaded case, are used to calculate θ , then a value of 1.1° is calculated for water loading. This is close agreement with the measured value. Thus phase angle is quite sensitive to changes in values for L and C . These two components can change in value from the effects of external temperature and pressure changes. These changes are then reflected in the phase angle measurement. Also, since Z_R is a complex value, the inductive or capacitive effects of the imaginary part can add to, or subtract from, the values of L and C and again affect the phase angle measurement.

Measurements of phase angle were made using a phase detector connected to a piezoelectric ceramic disc transducer when the transducer was immersed in several different media with various values of characteristic acoustic impedance. The ceramic disc was resonant at 55.2 kHz in air. Figure 17

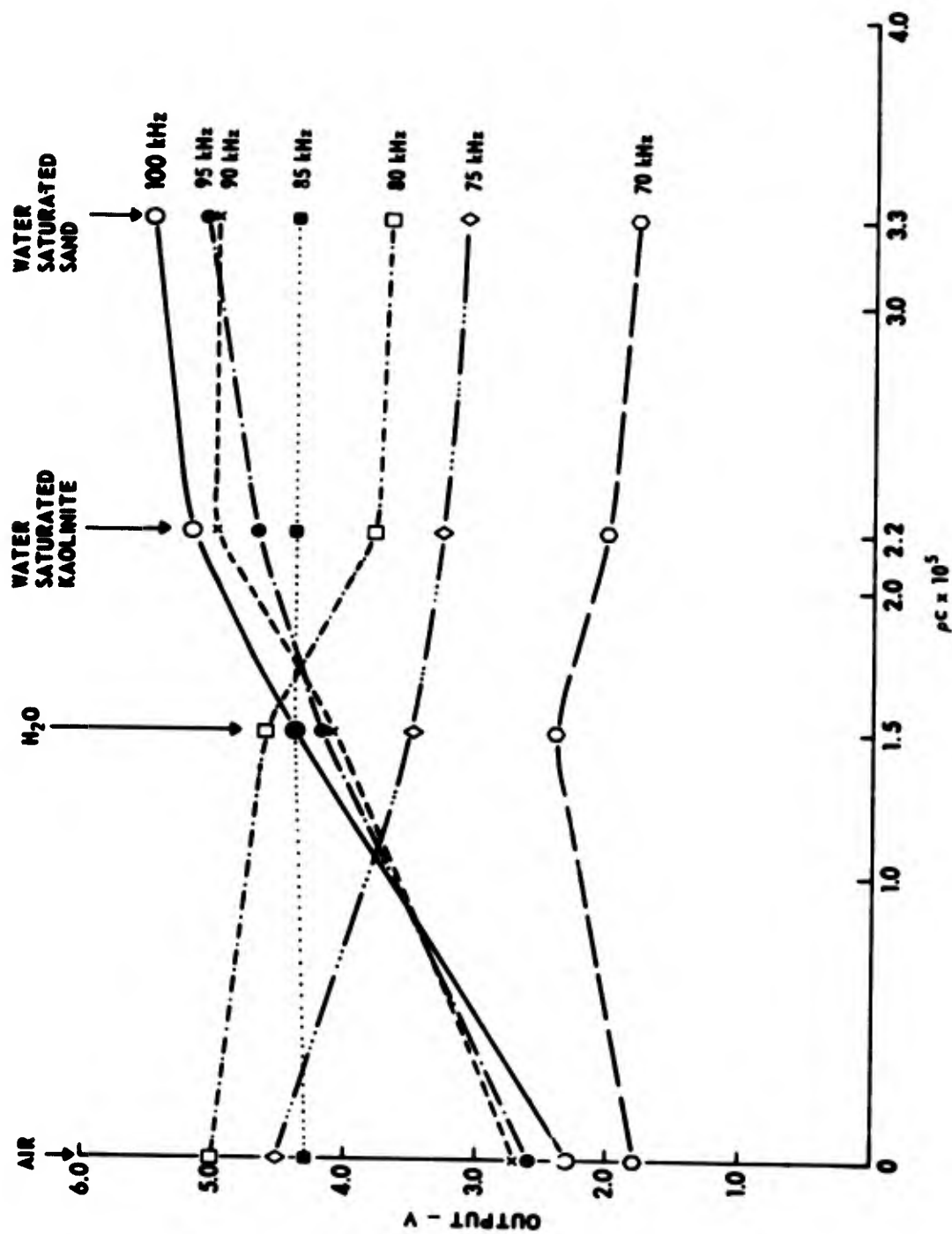


FIGURE 17
OUTPUT OF ACOUSTIC IMPEDANCE PROBE

ARL - UT
AS-75-1332
DJS - DR
10 - 3 - 75

shows plots of the output of the phase detector versus acoustic impedance for several frequencies. It is evident that the relationship of phase angle to acoustic impedance changes with changing frequency, as would be expected from the above equation for θ . At none of the frequencies is there a linear relationship, which indicates that the phase angle is changing due to parameters other than the radiation impedance. Figure 17 illustrates the sensitivity of this measurement to parameters other than acoustical radiation impedance of the medium.

An alternative method of measuring the radiation loading of a transducer is being studied. Since the diameter of the admittance circle is directly dependent on the radiation loading of the transducer, measurement of this diameter would provide a measurement of the radiation load. To make this measurement, the effects of the static capacitance C_0 must be eliminated by "tuning" the transducer with an inductance L_0 in parallel so that

$$\omega_0 = \frac{1}{L_0 C_0} ,$$

where ω_0 is the resonance frequency of the transducer. In such a case, the major diameter of the admittance circle lies on the G axis at resonance, Y is equal to G, and the phase angle θ is zero. Also, at resonance Y is related to R_L and R_R as follows,

$$Y = \frac{1}{R_L + R_R} .$$

Using this in the following expression,

$$I = EY ,$$

where I and E are the driving current and voltage respectively, then the current can be expressed as

$$I = \frac{E}{R_L + R_R} ,$$

which presents a more tractable relationship between a measurable parameter such as the current or voltage amplitude at the input of the transducer and its radiation load. A drawback to this method is that the resonance frequency of the transducer changes as the radiation loading changes so that the driving frequency must be changed to keep the phase angle at zero. Because the system must be operated in a pulsed mode to eliminate interference from boundaries, a complex electronic circuit is required. The schematic of Fig. 18 shows the system required for such a measurement. In the system, the phase-locked loop measures the phase between the voltage waveform and the current waveform of the transducer and varies its output frequency to keep the phase at zero. The output of the phase-locked loop is shaped by the pulse generator into a pulsed sinusoid. This pulse is amplified and maintained at a constant amplitude by the constant voltage amplifier (CVA). The CVA output is then applied to the transducer. Thus, because the voltage is constant and the phase is zero, the amplitude of the current waveform is a measure of the admittance of the transducer at resonance and is inversely proportional to the radiation resistance of the transducer. If the transducer aperture is much larger than a quarter wavelength, then the acoustic impedance of the medium can be considered real and can be measured by measuring the amplitude of the current waveform. A circuit based on this concept is being designed for further examination of the feasibility of in situ measurement of acoustical radiation resistance, and thus bulk density, of marine sediment.

D. Conclusion

One of the parameters of interest in characterizing a marine sediment is bulk density. Bulk density can be determined by removing a known volume of the material and weighing it. This procedure,

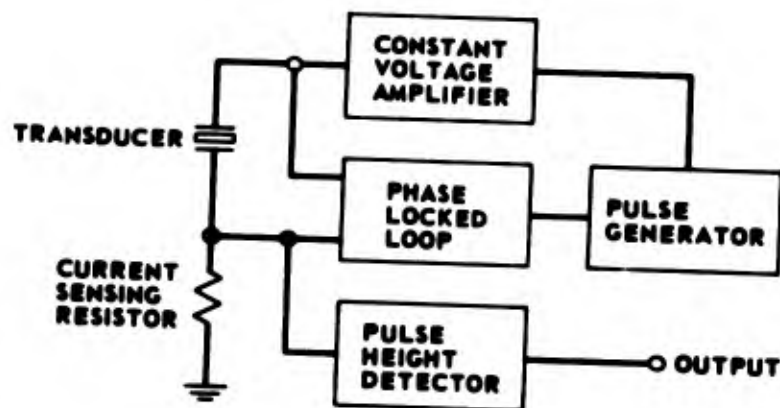


FIGURE 18
BLOCK DIAGRAM OF ACOUSTIC IMPEDANCE MEASURING CIRCUIT

however, tends to disturb the sediment and cause errors in parameter measurements. To eliminate these problems, minimum disturbance methods are needed for in situ measuring of bulk density. One method is to use the radiation loading of a driven transducer to measure the acoustical impedance of the material. Concurrent measurement of the compressional wave speed then allows the bulk density to be calculated. An easily measured parameter is the phase angle between the driving voltage and current waveforms to a transducer immersed in a sediment. This phase angle bears a relationship to the radiation loading on the transducer. Although the relationship is not linear, it has been shown that, with the proper selection of driving frequency, a usable output can be obtained from such a device.

Another, more difficult, measurement that can be made is the transducer driving current when the driving voltage is maintained constant and the transducer is kept at resonance by varying the driving frequency. Under these conditions, the amplitude of the current through the transducer bears a linear relationship to the acoustical impedance of the medium loading the transducer. Circuits to implement this measurement technique are being designed and constructed.

Acknowledgement

The application of equivalent circuit theory to the problem of ρc measurement was greatly aided by Mr. Reuben Wallace, who provided background information and computer programs.

IV. ENGINEERING PROPERTIES MEASUREMENT

A. Introduction

One reason for measuring the acoustical properties of ocean sediments is that the acoustic parameters have a direct relation to some of the engineering properties. In compressional wave work, direct relationships have been shown to exist between compressional wave speed and attenuation and such physical parameters as porosity, mean grain size, and bulk density (Akai, 1972; Hampton, 1967; Hamilton, 1973). Because it is important to understand how the engineering properties of a sediment affect its acoustic properties and because it is important to characterize a laboratory constructed sediment upon which acoustic measurements are made so that those measurements can be related to work done at other times and places, part of the research effort under the current program was aimed at developing a capability to measure several important engineering properties of sediments. Most analytic measurements such as porosity or grain size are made with ordinary laboratory equipment so that no special preparation was needed to make this type analysis. Two analyses did require construction of special equipment: Atterberg liquid limit and vane shear measurements. Construction of this equipment has already been described (Shirley and Anderson, 1975b).

In order to obtain as wide a range of parameters as possible, six different sediments were constructed. These consisted of a black carbonate clay with a carbonate content of 38%, kaolinite clay and a mixture of each of these two clays with 10% and 20% by weight of a fine silt obtained from a gravel washing operation.

Preceding page blank

Several engineering properties were determined for each of the sediments, among which are mean grain size, grain density, Atterberg liquid limit, Atterberg plastic limit, water content, bulk density, and vane shear strength. The parameters which are constant are summarized in Table II. The techniques used to measure the parameters are described separately below.

B. Grain Size

Two methods were used to measure the grain size distribution of the sediments: (a) dry sieve analysis for particle sizes down to 4 ϕ and (b) pipette analysis for particle sizes below 4 ϕ (see Folk, 1968). In the sieve analysis, a sample is dried, weighed, crushed, and then placed in a set of calibrated sieves. After a 15 min period of shaking, the material in each sieve is weighed. Material passing through the 4 ϕ sieve is used in the pipette analysis. In the pipette analysis, the sediment sample is dispersed in 1000 ml of water containing a dispersing agent (Calgon) to prevent flocculation. As the mineral grains slowly settle through the water column, specified volumes of the water-sediment mixture are removed by pipette at a specified depth in the liquid. These samples are oven dried and weighed to determine the weight of mineral grains in that particular volume. Because each range of grain sizes will have its own settling time to a certain depth, then the grain size can be determined from the weight of material in the samples.

Figures 19 and 20 show the grain size distributions found for the six sediments. Figure 19 shows the data for the three sediments with the black carbonate clay as the main constituent, while Fig. 20 shows the data for the three kaolinite clay sediments. The percentage ratio of clay to silt is only approximate in each case.

TABLE II

Sediment Type	Mean Grain Size	Grain Mineral Density	Atterberg Liquid Limit	Atterberg Plastic Limit
Pure Kaolinite	8.1φ	2.52	28.82	23.0%
Kaolinite and 10% silt	8.0φ	2.57	24.2	21.8
Kaolinite and 20% silt	7.2φ	2.62	21.5	18.6
Pure Black Clay	9.4φ	2.42	45.1	26.1
Black Clay and 10% silt	7.9φ	2.47	42.5	21.0
Black Clay and 20% silt	7.2φ	2.50	37.9	19.4
Silt	4.8φ	2.74	—	—

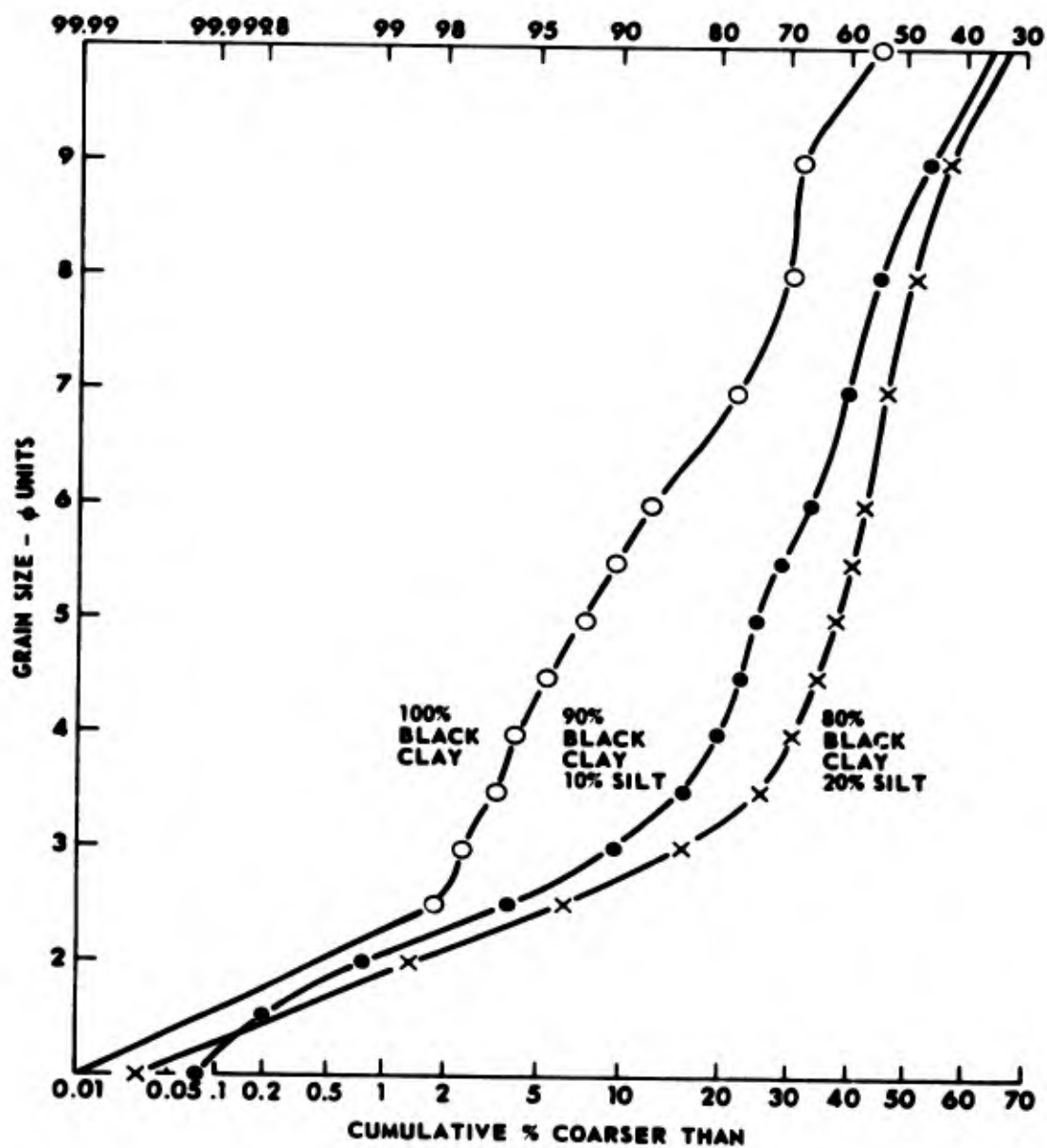


FIGURE 19
GRAIN SIZE DISTRIBUTION FOR BLACK CLAY SEDIMENTS

ARL - UT
AS-75-1334
DJS - DR
10 - 3 - 75

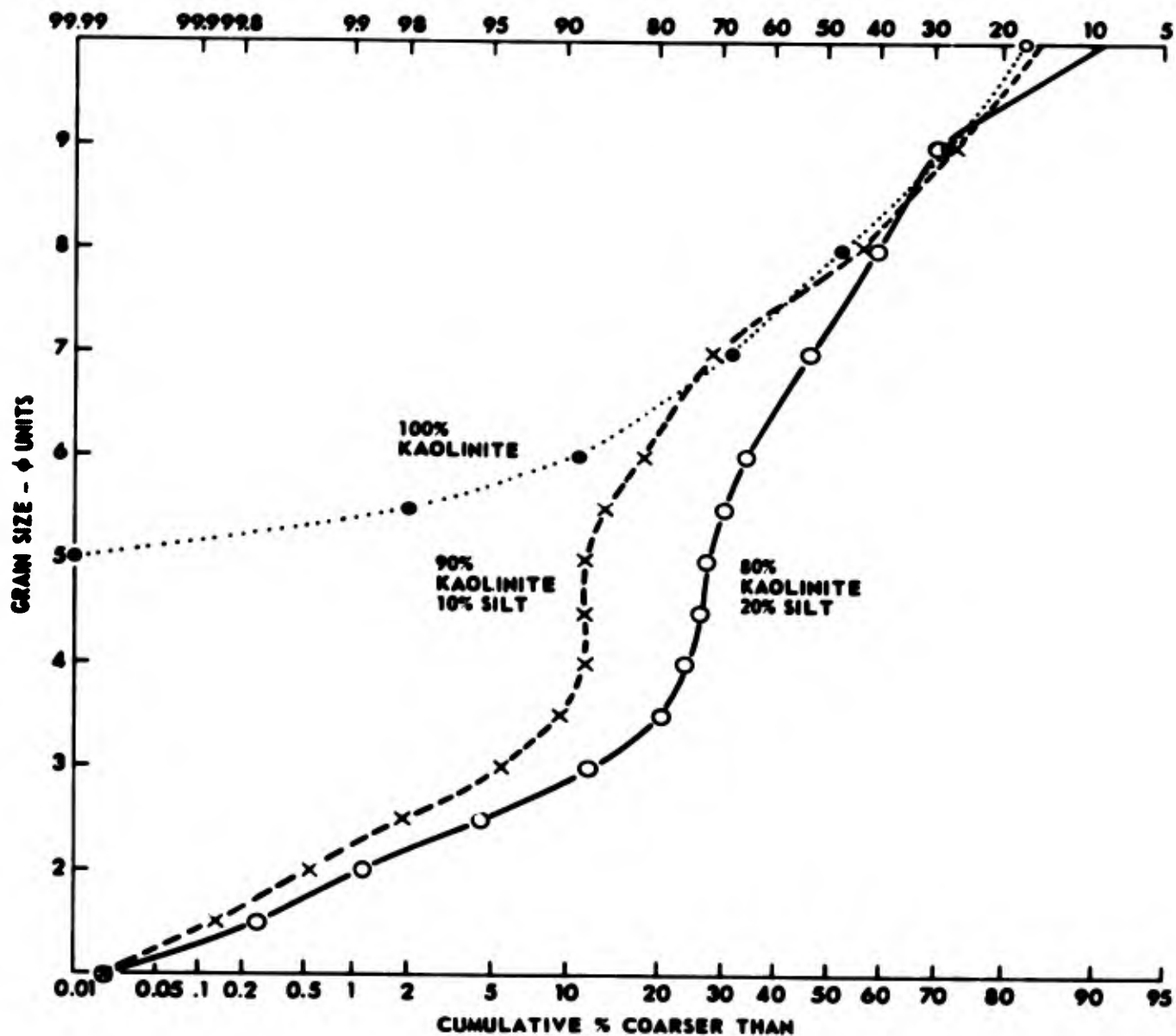


FIGURE 20
GRAIN SIZE DISTRIBUTION FOR KAOLINITE SEDIMENTS

ARL - UT
AS-75-1335
DJS - DR
10 - 3 - 75

C. Porosity and Bulk Density

Porosity, defined as the ratio of the volume of voids to the volume of solids, is calculated from the weight percentage of water for fresh water sediments. Water content is determined by weighing a sample of wet sediment, oven drying the sediment at 105°C, and then reweighing it. The percent that was water is calculated from the weight loss of the dried sample.

Bulk density can be determined in one of two ways. Determination of the weight of an accurately measured volume of wet sample gives the bulk density directly. If the density of the mineral grain is known, bulk density can also be calculated from water content.

D. Atterberg Limits

The two Atterberg limits that are of principal interest are the liquid limit, defined as the water content at the point that the sediment ceases to be a liquid, and the plastic limit, defined as the water content at which the sediment is no longer plastic. Determination of the liquid limit requires that the sample be placed in a small hemispherical cup, a standard size groove cut in the sediment, and the cup pounded on a solid base at a constant rate until the groove starts to close. The water content of the sample when it requires 25 blows to close the groove is defined as the liquid limit.

The plastic limit is determined by rolling a small sample of sediment into a thin thread. The plastic limit is defined as the water content of the sample when a 1/8 in. diam thread starts to break up into small pieces (of 1/8 in. to 1/2 in. in length).

The values of the Atterberg limits for the six sediments are listed in Table I; see page 38.

E. Vane Shear Strength

Vane shear strength of a sediment is determined by measuring the maximum torque exerted on a 4-bladed vane rotated in the sediment at a constant angular velocity. Figure 21 shows a schematic drawing of the device that was constructed to measure the vane shear strength of sediments. A small synchronous gear motor turns a shaft at the recommended rate of 6° per minute. Torque on the shaft is measured by a strain gauge bridge. The bridge is rigidly mounted on a thin flat crosspiece which transfers the rotational force from a yoke on the motor shaft to the shaft carrying the vane blades. Torque exerted by the motor and resisted by the sediment around the vane causes the crosspiece to bend and thus causes an imbalance of the strain gauge bridge. Two sets of vanes were constructed. One set has an outside diameter of 2.0 cm and a height of 1.8 cm; the other set has a 4.0 cm o.d. and a 2.0 cm height.

Figure 22 shows the output of the torque sensor plotted versus vane angle for the 20% silt, 80% kaolinite sediment that had 25.8% water content. These curves are typical for many of the determinations. The torque rises steeply at first. After a change in the rate of increase (change in the slope of the plot), the torque reaches a maximum and then gradually decreases. In a few of the measurements, the torque curve did not decrease after the change in slope but rather continued a gradual increase. In these cases the maximum torque, for the present calculations of shear strength, was taken as the value on the curve just after the initial change in slope. Shear strength determinations at levels of water content were made on each of the six sediments. The samples were allowed to air dry over a period of time, water content was determined, and vane shear strength was measured. Figure 23 shows vane shear strength for each of the six sediments plotted versus water content. Circled points indicate data taken using the 2 cm diam vane, while points in triangles indicate data from the 4 cm diam vane. Torque values were converted to shear strength values by the following equation (Monney, 1974):

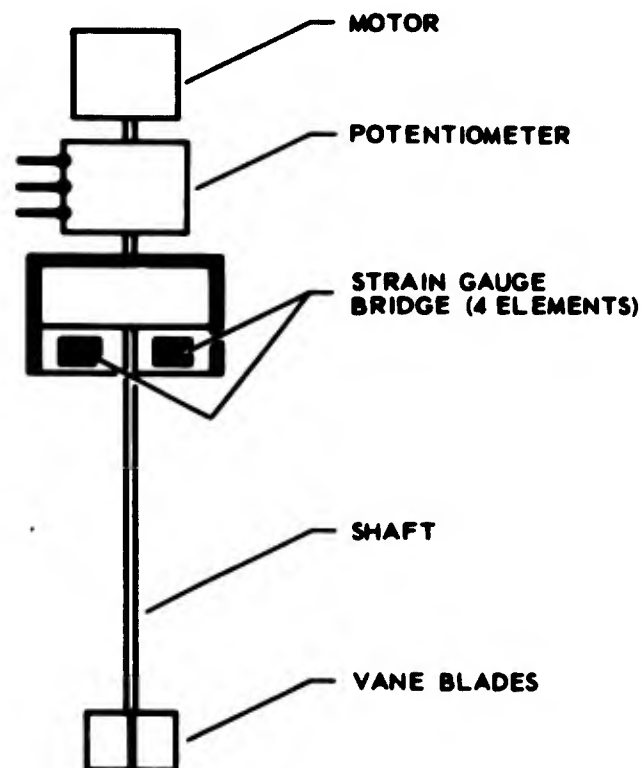


FIGURE 21
SCHEMATIC REPRESENTATION
OF VANE SHEAR APPARATUS

ARL - UT
AS-75-489
DJS - DR
4 - 3 - 75

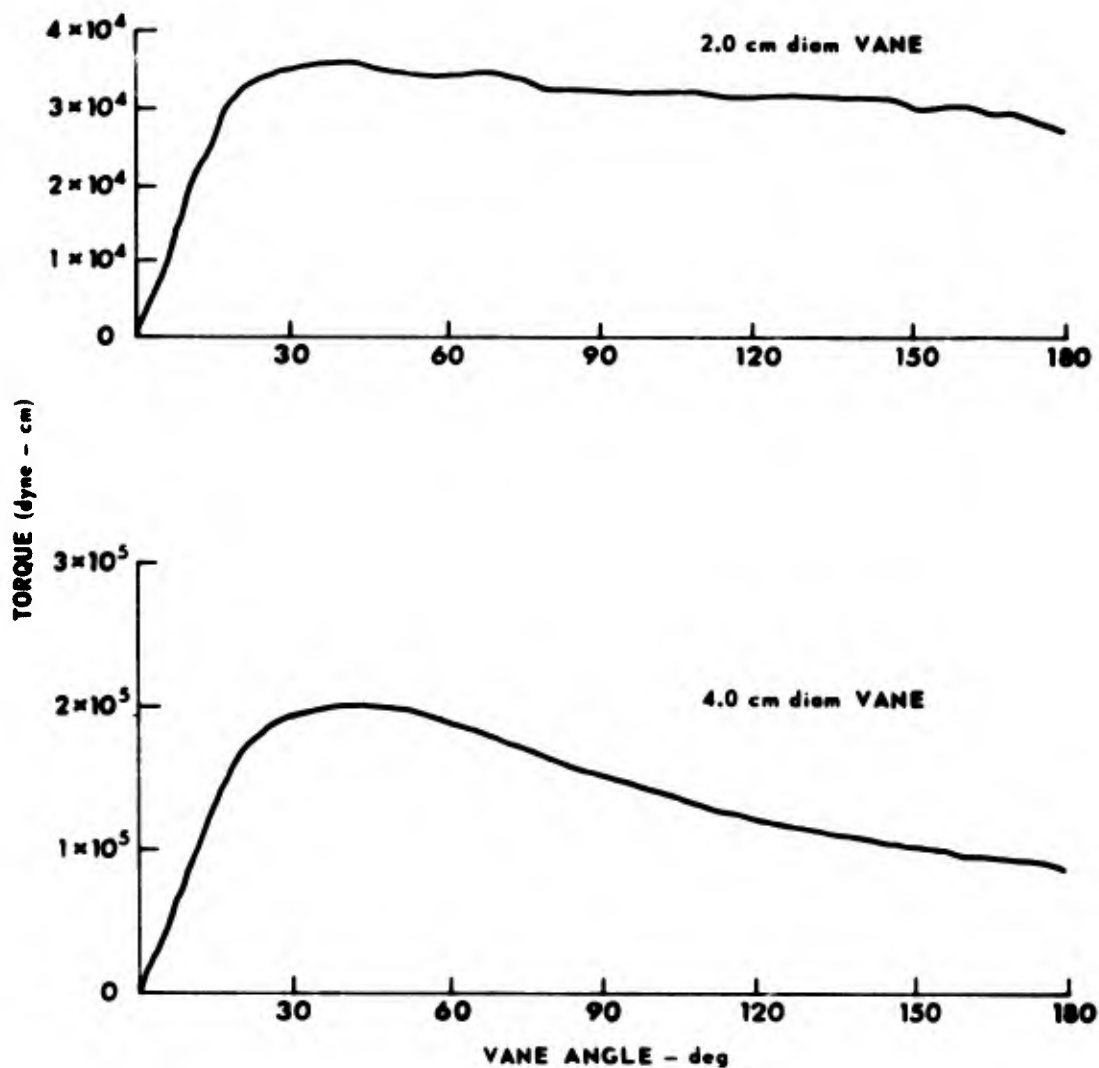


FIGURE 22
VANE SHEAR STRENGTH OF 80% KAOLINITE - 20% SILT AT 25.8% WATER

ARL - UT
 AS-75-1336
 DJS - DR
 10 - 3 - 75

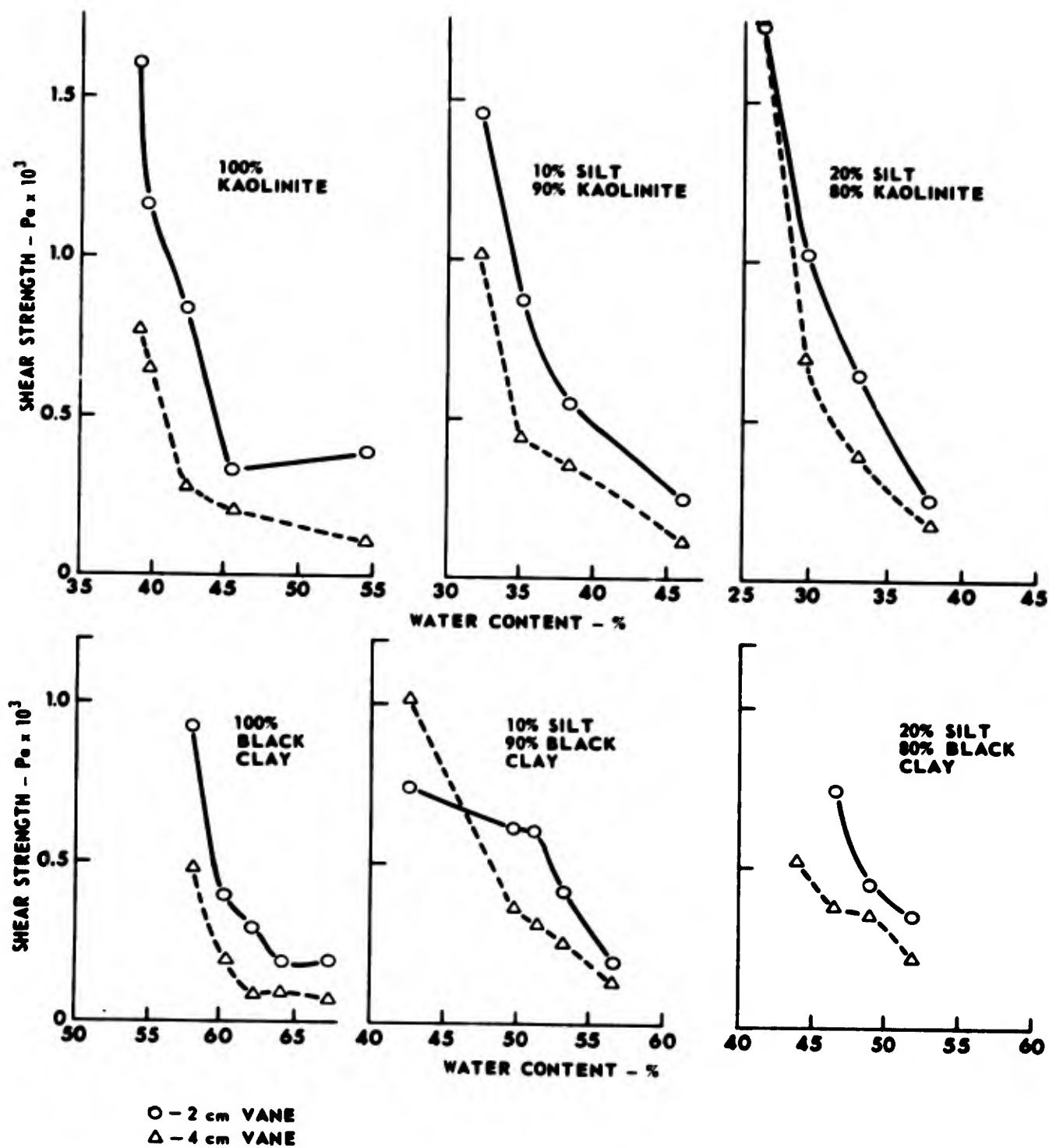


FIGURE 23
VANE SHEAR STRENGTHS FOR LABORATORY SEDIMENTS

ARL - UT
AS-75-1337
DJS - DR
10 - 3 - 75

$$S = \frac{T}{\pi(H \frac{D^2}{2} + \frac{D^3}{6})} ,$$

where

S - shear strength,

T - torque,

H - height of vane blades, and

D - diameter of vane blades.

The derivation of this equation is shown in Appendix I. Although the 4 cm vane gave more consistent results, the shear strength values for the 4 cm vane were consistently lower than those for the 2 cm vane. This finding is possibly due to the fact that, although the vane rotation rate was the same in each case, the larger diameter of the 4 cm vanes caused the shearing surfaces to move faster, and consequently did not allow as much rebonding of sediment grains.

F. Conclusion

For an effective program of acoustic investigation of the properties of natural and laboratory sediments, one must be able to characterize the physical properties of those sediments so that results can be related to other work on a larger variety of sediments. Toward this end, the capability of measuring various engineering properties has been developed as a necessary adjunct to the acoustics program.

V. SUMMARY

This report describes an ongoing program at ARL/UT; the work, supported under Contract N00014-70-A-0166, Task 0017, has the following objectives:

- 1) in situ measurement of compressional wave speed and attenuation in ocean sediments,
- 2) in situ measurement of shear wave speed and attenuation in ocean sediments,
- 3) in situ measurement of bulk density in ocean sediments, and
- 4) correlation of the above acoustic parameters with engineering properties of the sediments.

The first of the above objectives has been reached; a compressional wave profilometer has been developed that is capable of obtaining in situ compressional wave speed and attenuation profiles of ocean bottom sediments in water depths to 5 km. The profilometer was developed in the following stages.

- 1) A preliminary laboratory investigation was conducted to confirm that compressional wave sound speed could be measured while coring. Previously developed transducer and laboratory type electronic equipment were used in this stage.
- 2) Field tests were performed, still utilizing laboratory type electronic equipment, to confirm that results could be obtained in an actual working situation.
- 3) Electronics equipment were designed and constructed to replace the laboratory type equipment and to allow operation under more realistic conditions in deep water.
- 4) Field tests of the final equipment design in which data were taken during normal coring operations in deep oceanic waters. The equipment is now routinely used in other coring programs.

Preceding page blank

The second part of the program, which is concerned with shear wave measurements, is in the first stage of development. Unlike the compressional wave measurements which could use previously developed transducer technology, shear wave work in the laboratory stage required that transducers capable of making the measurements be developed. Since transducers have now been developed which can measure shear wave parameters in soft sediments (shear moduli $\sim 10^5$ dynes/cm²), work is now progressing toward the completion of stage one and the beginning of stage two, in which field tests will be performed. Stage 3 for shear waves will require less effort than for compressional waves because most of the electronics circuits developed to measure compressional wave parameters can be modified to measure shear wave parameters.

The acoustical measurement of bulk density is also in the first stage of development. Thorough investigation has revealed that the measurement of phase angle between the current and voltage waveforms of a drive transducer can be used to determine radiation impedance. However, this technique is less desirable than other measurement methods under investigation because of interactions of other parameters of the medium.

Because the determination of engineering properties requires only previously developed technology and because no effort is being expended in this program to measure these parameters in situ, only the first stage of development is required for this task. As sediments are obtained and utilized in the acoustics part of the program, their engineering properties will be determined for comparison and correlation with their acoustic properties.

The accomplishments to date in the program are:

- 1) routine determination of profiles of compressional wave speed and attenuation in deep water sediments,
- 2) development of shear wave transducers capable of measuring shear wave speed and attenuation over a 10 cm path at frequencies as low as 200 Hz,

- 3) development of the capability to make both compressional and shear wave measurements over the same path at the same time,
- 4) preliminary investigation of a device to measure bulk density in situ by acoustic means, and
- 5) development of the capability to measure engineering properties of sediments used in the acoustics program.

APPENDIX I

To derive sediment shear strength from the torque applied to the vane blades in a vane shear apparatus, the following assumptions (Monney, 1974) are made.

- 1) The failure surface is a right circular cylinder with radius equal to the width of the vane blades and with length equal to the height of the blades.
- 2) The stress distribution is everywhere equal and uniform on the surface of the cylinder at maximum torque.

The shear strength is defined as the shear stress at failure of the sediment in shear. The shear stress, s , is the force per unit area applied parallel to that area:

$$\frac{1}{S} \int_A \frac{dA}{F} ,$$

where

F = force, and

A = area.

For the sides of the cylinder, the force is everywhere constant and equal to the torque divided by the radius $D/2$ so that

$$\frac{1}{S_1} = \frac{1}{F} \int_A dA = \frac{AD}{2T} .$$

Since the area, A , of the side of the cylinder is given by

$$A = \pi DH ,$$

where H = height of cylinder, then the expression for S_1 becomes

Preceding page blank 63

$$\frac{1}{S_1} = \frac{\pi H \frac{D^2}{2}}{T} \quad .$$

For the top and bottom of the cylinder, let dA be an annulus of area $dA=2\pi r dr$, so that

$$\frac{1}{S_2} = \int_0^R \frac{2\pi r dr}{F(r)} \quad .$$

Since force is equal to torque divided by radius, the force applied to the annulus at a radius r is

$$F(r) = \frac{T}{R} \quad .$$

Thus, S_2 can be written

$$\frac{1}{S_2} = \int_0^{D/2} \frac{2\pi r^2 dr}{T} \quad ,$$

which, upon integration, yields

$$\frac{1}{S_2} = \frac{\frac{2}{3} \pi \frac{D^3}{8}}{T} = \frac{\pi \frac{D^3}{12}}{T} \quad ,$$

so that S_2 is given by

$$S_2 = \frac{T}{\pi \frac{D^3}{12}} \quad .$$

Because there are two ends of the cylinder, then the total shear stress is given by

$$\frac{1}{S} = \frac{1}{S_1} + \frac{1}{2S_2} \quad ,$$

which, from the above expressions for S_1 and S_2 , can be written

$$\frac{1}{S} = \frac{\pi H \frac{D^2}{2} + \pi \frac{D^3}{6}}{T} \quad .$$

Inverting this expression yields the following

$$S = \frac{T}{\pi(H \frac{D^2}{2} + \frac{D^3}{6})} \quad .$$

This is the expression used to relate the measured torque to sediment shear strength in section IV of this report.

BIBLIOGRAPHY

- Akal, T., "The relationship between the physical properties of underwater sediments that affect bottom reflection," Marine Geology 13, 251-266, 1972.
- Anderson, A. L., "Acoustics of Gas-Bearing Sediments," Applied Research Laboratories Technical Report No. 74-19 (ARL-TR-74-19), Applied Research Laboratories, The University of Texas at Austin, Austin, Texas, 1974.
- Folk, R. L., Petrology of Sedimentary Rocks (Hemphills, Austin, Texas, 1968).
- Hamilton, E. L., "Prediction of deep sea sediment properties: state of the art," Deep Sea Sediments: Physical and Mechanical Properties, A. L. Inderbitzen (ed.), (Plenum Press, New York, 1974).
- Hampton, L. D., "Acoustic properties of sediments," J. Acoust. Soc. Am. 42, 882-890 (1967).
- Hueter, T. F., and R. H. Bolt, Sonics (John Wiley & Sons, New York, 1955).
- Monney, N. T., "An analysis of the vane shear test at varying rates of shear," Deep Sea Sediments: Physical and Mechanical Properties, A. L. Inderbitzen (ed.), (Plenum Press, New York, 1974).
- Preiss, K., "Non-destructive laboratory measurement of marine sediment density in a core barrel using gamma radiation," Deep-Sea Research 15, 401-407, 1968a.
- Preiss, K., "In situ measurement of marine sediment density by gamma radiation," Deep-Sea Research 15, 637-641, 1968b.
- Shirley, D. J., and L. D. Hampton, "Acoustic Velocity Profilometer for Sediment Cores," OCEAN '72 Record of the International Conference on Engineering in the Ocean Environment, Newport, Rhode Island, 13-15 September 1972.
- Shirley, D. J., A. L. Anderson, and L. D. Hampton, "Measurement of in-situ Sound Speed during Sediment Coring," OCEAN '73 Record of the International Conference on Engineering in the Ocean Environment, Seattle, Washington, 25-28 September 1973.

Preceding page blank

BIBLIOGRAPHY (Cont'd)

Shirley, D. J., and A. L. Anderson, "Compressional Wave Profilometer for Deep Water Measurements," Applied Research Laboratories Technical Report No. 74-51 (ARL-TR-74-51), Applied Research Laboratories, The University of Texas at Austin, Austin, Texas, 1974.

Shirley, D. J., and A. L. Anderson, "Studies of Sediment Shear Waves, Acoustical Impedance, and Engineering Properties," Applied Research Laboratories Technical Report No. 75-23 (ARL-TR-75-23), Applied Research Laboratories, The University of Texas at Austin, Austin, Texas, 1975.